Title

Development of an Ecological Model Incorporating Benthic Processes in an Unsteady Framework

Authors

Breithaupt, Stephen A
King, Ian P
Orlob, Gerald T

Publication Date

1995

DEVELOPMENT OF AN ECOLOGICAL MODEL INCORPORATING BENTHIC PROCESSES IN AN UNSTEADY FRAMEWORK

By
Stephen A. Breithaupt, Ian P. King, and Gerald T. Orlob
Department of Civil and Environmental Engineering
University of California
Davis, California 95616

TECHNICAL COMPLETION REPORT

Project Number UCAL-WRC-W-792
January, 1995

University of California Water Resources Center

The research leading to this report was supported by the University of California, Water Resources Center, as part of Water Resources Center Project UCAL-WRC-W-792

TABLE OF CONTENTS

LIST OF FIGURES

LIST OF TABLES

ABSTRACT

An ecological model incorporating benthic algae was developed using an existing unsteady one and two-dimensional water quality model (RMA-4q) to transport constituents in the water column. The types of benthic algae simulated are attached filamentous algae (e.g. *Cladophora*) and perilithic biofilm. These are influenced by different physical processes, although hydrodynamic detachment occurs with each. Attached filamentous algae occur in the turbulent flow region and access to nutrients is assumed not to be limited by diffusion, as is the case for perilithic biofilms. The biofilm equation solution is therefore more difficult to solve. The theoretical development of the equations for each benthic algal type is presented, along with numerical solution schemes. Field data collection methods and their results are discussed. The data are used in support of the modeling effort. Finally, results from an example application for the Russian River are given. The effect of nutrient loading and hydrodynamic detachment are evident. Problems with temperature and its relation to system geometry are discussed. Topics for future research are presented.

Keywords: algae, benthos, finite element method, numerical modeling, nitrogen, nutrients, phosphorus, river beds, water quality, water quality modeling

INTRODUCTION

BACKGROUND

In many natural waters benthic processes regulate the interactions of water quality constituents (from DO production/consumption to concentration of toxics). Frequently, water quality models ignored benthic processes or considered them as source/sink terms. If considered as sources or sinks, the process rates are specified by the model user; the processes occurring in or on the benthos are not explicitly modeled. Thus the focus of most existing models has been primarily on the water column. Those which do have a benthic are either not comprehensive (consider only one process or constituent, particularly phosphorus) and/or have a simplified hydrodynamic component.

Natural waters are in a constant state of hydrodynamic, chemical and biological flux. Staff of regulatory agencies such at the California Regional Water Quality Control Board have expressed concern about benthic nutrient cycling and excessive benthic algae growth in streams and rivers. To properly represent and manage these types of waters a model must consider all the processes which are important to the problem at hand. An unsteady hydrodynamic model is a necessary framework upon which to improve modeling capabilities and our understanding of these processes. Because of the paucity of models involving benthic processes in conjunction with unsteady hydrodynamics and water quality processes in the overlying water column, water quality managers do not have available the most appropriate tools to evaluate management alternatives. While some models are available which describe sediment processes, they are considered separately from the other processes affecting water quality, particularly hydrodynamics.

PROJECT SCOPE AND OBJECTIVES

This project was designed to develop a comprehensive water quality model which combines water column water quality and ecological reactions with the important benthic processes on the bed. The existing unsteady hydrodynamic/water quality framework represented by RMA-2 and RMA-4q was selected for this extension[1]. A new modeling framework has been created from the RMA-4q model so that additional processes in the bed, the water column or in the immediate atmosphere above, can easily be added.

Theoretical and numerical analysis has been focused on the development of relationships that describe the growth and attachment of benthic algae. Two types of benthic algae have been analyzed: filamentous algae (particularly *Cladophora*) and the perilithic biofilm.

It was recognized during the theoretical development that little or no data were available to describe the parameters needed for modeling. As a consequence efforts in this project were redirected to add a field work component. Specifically fieldwork was undertaken to quantify the biomass and characteristics of both benthic alga forms. Middle and lower

[1] See the Russian River modeling section for more description of the transport model.

reaches of the Russian River were selected for this these measurements. This data is now available as a resource to evaluate model performance.

REPORT ORGANIZATION

A detailed literature review is presented and describes approaches used in previous water quality models. The focus of this review is on modeling methods for filamentous and perilithic algae. Equations used by earlier researchers are presented to provide a basis for the later chapters of this report. The experimental section gives methods used and the results obtained. New models for both algae types are presented in the model development section. Starting with theoretical developments, this section also presents the development of the numerical algorithm for solution. A sample application is given in the Russian River modeling section. Using typical parameter values for *Cladophora* with a varying hydraulic and water quality regime, the model output is discussed for key constituents. Finally, conclusions of the research are presented and suggestions for future study are offered.

LITERATURE REVIEW

MODELING FILAMENTOUS ALGAE

BIOLOGICAL GROWTH EQUATIONS

Smith (1978) reports on a benthic algae routine used in WQRRS. This routine is described in the users manual for the model, without any applications examining the modeled processes. The growth equation used is as follows:

$$\frac{\partial BA}{\partial t} = BA(BAG - BAR) - BAPRED - BSCOUR \qquad (1)$$

where BA = concentration of benthic algae (g m^{-2}), BAR = benthic algae respiration rate (day^{-1}), and BAPRED = grazing rate by aquatic invertebrates and fish (g m^{-2} day^{-1}). The other terms are described below. The growth term (BAG; day^{-1}) considers the minimum of either a light or critical nutrient factor, that are computed using the Monod relationship.

$$BAG = BAMAX * \min\left[\left(\frac{C}{C_2 + C}\right),\left(\frac{LI}{LI_2 + LI}\right)\right] \qquad (2)$$

with BAMAX = benthic algae's maximum growth rate (day^{-1}), C = concentration of some limiting nutrient (mg L^{-1}), LI = light intensity (langleys), and C_2 and LI_2 are the half-saturation constants for nutrient and light, respectively. Losses of benthic algae are from respiration, grazing, and scour. Scour is described by the following equation;

$$BSCOUR = SK * VEL^2 \qquad (3)$$

with BSCOUR = scour rate (mg m^{-2} day^{-1}) SK = scour coefficient (mg m^{-2} day^{-1} $(m/s)^{-2}$) and VEL = stream velocity (m s^{-1}). Equation 3 is related to the equation for drag and considers no critical velocity below which scour is negligible. It can be seen in equation 1, that scour is also not a function of the biomass present at any time.

The SSAM-iv model includes a benthic algae component that is influenced by nutrient concentration in the water column, density of growth, mortality, and scour (Grenney and Kraszewski, 1981). Nutrient limitation is modeled as the minimum of the nitrogen or phosphorus growth factor computed from Michaelis-Menton kinetics. The nitrogen growth factor is modified allowing for preference for ammonia or nitrate to be specified. The general equation is as follows:

$$\frac{\partial PX_B}{\partial t} = \Phi P \qquad (4)$$

where P = wetted perimeter of stream (m) and X_B = density of benthic algae (g m^{-2}). The net growth rate Φ (g m^{-2}-sec^{-1}) has the following form:

$$\Phi = \left\{ \mu \left[\frac{g - X_B}{g} \right] - \tau\beta_1 - \beta_2 V \right\} X_B \qquad (5)$$

where μ = specific growth rate (sec^{-1}), τ = dimensionless temperature adjustment factor, β_1 = death rate (sec^{-1}), V = stream velocity (m s^{-1}). β_2 is the scour rate, that relates detachment to the stream velocity. It has units as follows:

$$\frac{\text{rate}/\text{mass}}{\text{velocity}} \equiv \frac{g/s/g}{m/s} \equiv m^{-1}.$$

They estimate β_2 to have a range between $1x10^{-6}$ and $1x10^{-5}$ m^{-1}, but state that not enough research has been done to provide good estimates. The specific growth rate μ is computed using Michaelis-Menton kinetics for phosphorus and nitrogen.

Grenney and Kraszewski (1981) solve a steady-state form of equation 4. Of course, at steady-state,

$$\frac{\partial P X_B}{\partial t} = 0, \qquad (6)$$

so that the remaining terms can be solved for X, giving

$$X_B = \frac{g(\mu - \tau\beta_1 - \beta_2 V)}{\mu}. \qquad (7)$$

The steady-state solution is the balance between nutrient limited growth and the loss terms (mortality and scour). This equation still contains the non-linear term μ and as such increases the difficulty in solving the system.

In 1982, a series of articles were published dealing with the growth of *Cladophora glomerata*, a filamentous green algae, in Lake Huron. *Cladophora* attaches to the substrate of freshwater systems. In these articles, field, laboratory, and modeling work is discussed. Canale and Auer (1982e) discuss model development and calibration. In this they describe changes in *Cladophora* biomass by

$$\frac{dX}{dt} = [\mu - R - L]X, \qquad (8)$$

with X = biomass density (gm m^{-2}), μ = gross growth rate (day^{-1}), R = respiration rate (day^{-1}), and L = sloughing loss rate (day^{-1}). Gross growth rate is governed by the

maximum specific growth rate (μ_{max}; day^{-1}) and dimensionless multipliers accounting for light (M_L), phosphorus (M_P), and habitat limitations (M_X), i.e.,

$$\mu = \mu_{max}\left[M_L M_P M_X\right]. \tag{9}$$

Auer and Canale (1982c) state that the Monod model does not adequately describe *Cladophora* growth rate, because it is driven by the internal rather than external nutrient levels. It is the phosphorus multiplier that incorporates internal phosphorus levels. Their approach is described by the following equation

$$M_p = 1 - \frac{Q_o}{Q}. \tag{10}$$

Q_o is the minimum cell phosphorus level required for growth and was found to be 0.05%P for *Cladophora* in the study site on Lake Huron, Michigan. The internal phosphorus level (Q, units of %P) is a dynamic relation between uptake rate (ρ, units of %P-day^{-1}) and utilization for growth and is described by

$$\frac{dQ}{dt} = \rho - \mu Q. \tag{11}$$

Finally, the uptake rate is described by a relation between external phosphorus levels (P) and the amount of internal phosphorus above the minimum. This takes the following form

$$\rho = \rho_{max}\tau\left[\left(\frac{P}{K_e + P}\right)\left(\frac{K_q}{K_q + Q - Q_o}\right)\right]. \tag{12}$$

Equation 12 describes phosphorus uptake by competitive enzyme inhibition (Auer and Canale, 1982b) with ρ_{max} = maximum uptake rate (%P day^{-1}), τ = dimensionless temperature correction factor, P = external phosphorus concentration ($\mu g\ P\ L^{-1}$), K_e = half-saturation constant for external phosphorus uptake ($\mu g\ P\ L^{-1}$), and K_q = phosphorus uptake inhibition constant (%P). For $P >> K_e$ and $Q \cong Q_o$, ρ approaches ρ_{max}. This would be the situation where phosphorus depleted cells are exposed to a high concentration of phosphorus. As $Q - Q_o$ increases, ρ will decrease indicating increased internal phosphorus pool size reduces the uptake rate. From equation 11, Q will be reduced as the growth rate increases.

Canale and Auer (1982e) accounted for sloughing losses in equation 8 through the use of an empirical relation between wind speed and biomass density. Since they were modeling *Cladophora* in Lake Huron, they assumed that wave induced velocity was proportional to wind speed. Presumably they see sloughing as caused by shear stress

acting on the algal mass; since they correct for the effect of sampling cages on shear stress. Their empirical relation is as follows

$$L = c_\tau L_{max} \frac{\omega}{\omega_{max}} \frac{X}{X_{max}}. \qquad (13)$$

Here c_τ = dimensionless shear stress correction factor (= 3.4), L_{max} = maximum sloughing loss rate (= 0.176 day^{-1}), ω = wind speed (mph), ω_{max} = maximum wind speed (= 11.1 mph), and X_{max} = maximum biomass density (= 433 g m^{-2}). Since L = L(X), substituting 13 into 8 yields a non-linear equation.

None of the models described above consider the effect of a diffusion layer surrounding the filament. Novotny (1969) discusses the effect of hydraulic parameters on the existence of a diffusion boundary layer adjacent to solids boundaries. This diffusion layer could be a limiting factor if the flux across this layer is less than the reaction rate within the solid. However, Krenkel and Thackston (1969) state in regard to *Sphaerotilus*, which grows in filaments in heavily polluted water , that its filaments may extend into the turbulent zone. Then the diffusion layer's depth would be determined by the arrangement of filaments, or it may even be stripped off.

Observation of filamentous algae in flowing waters shows it undulates as it streams behind the point of attachment. Presumably the undulations are a result of vortex shedding from the solid boundary, indicating the presence of a turbulence regime in the vicinity of the filament. From the research discussed above, there was no discussion of the relevance of a diffusion layer adjacent to the filaments. Hence, an implicit assumption of those models is there is no such layer that could impinge on the rate of nutrient utilization. The effect of the diffusion layer is to regulate the concentration of material at the surface of the solid, based on the materials diffusion coefficient in water, the thickness of the layer, and the material's concentration gradient. This is discussed in more detail below.

INTERACTIONS WITH THE WATER COLUMN

Typical interactions of filamentous algae with the water column involve the uptake of dissolved phosphorus, ammonia nitrogen, and nitrate nitrogen. Algae also produce oxygen, that can enter the water column or, if production rates are very high, could produce bubbles which exit to the water surface.

Considering only the algae-water column interactions that Smith (1978) included, they take the following forms for phosphate phosphorus, ammonia nitrogen, nitrate nitrogen, and dissolved oxygen:

$$\frac{dPO_4}{dt} = -\sum A \cdot AP(AG - AR)$$
$$\frac{dNH_3}{dt} = -\sum A \cdot AN(AG \cdot FNN - AR)$$
$$\frac{dNO_3}{dt} = -\sum A \cdot AN \cdot AG(1 - FNN) \qquad (14)$$
$$\frac{dO_2}{dt} = \sum A(O_2P \cdot AG - O_2R \cdot AR)$$

These are the source/sink terms that appear in the general transport equation. Here the summation is done over both algal forms, phytoplankton and benthic algae, so that A = concentration for both benthic algae and phytoplankton, AP = phosphorus fraction of algae (g P g algae^{-1}), AG = algal growth rate (day^{-1}), AR = algal respiration rate (day^{-1}), AN = nitrogen fraction of algae (g N g algae^{-1}), FNN = fraction of ammonia used for algal growth, O_2P = stoichiometry between oxygen production and algal growth (g O_2 g algae^{-1}), and O_2R = stoichiometry between oxygen production and algal respiration (g O_2 g algae^{-1}). Note for benthic algae, the rate for each constituent in 14 should be divided by the depth to distribute it over the water column.

For phosphorus and ammonia, the net change is a function of growth rate which results in a loss from the water column, hence the minus sign, and respiration. Respiration includes mortality and cell maintenance. The uptake or loss of nutrient is assumed to occur in direct proportion to the cell's stoichiometry. For nitrogen use in algal growth, there may be a preference for either ammonia or nitrate. Finally, algae produce and consume oxygen in proportion to their growth and respiration rates, respectively. The production proportion (O_2P) also reflect the amount of oxygen dissolved and not the amount which exits to the water surface.

Grenney and Kraszewski (1981) have similar functions describing benthic algae interactions with the water column. The benthic algae and phytoplankton source/sink terms take the following forms:

$$\phi_{DP} = -\beta_{B,P} \frac{\mu_B(g - X_B)}{gR} X_B$$
$$\phi_{NH3} = -\beta_{B,NH3}\alpha_B \frac{\mu_B(g - X_B)}{gR} X_B$$
$$\phi_{NO3} = -\beta_{B,NO3}(1 - \alpha_B)\frac{\mu_B(g - X_B)}{gR} X_B \qquad (15)$$
$$\phi_{O_2} = \beta_{B,O_2} \frac{\mu_B(g - X_B)}{gR} X_B$$

ϕ_* are the rate terms for dissolved phosphorus, ammonia and nitrate nitrogen, and dissolved oxygen (sec^{-1}). $\beta_{B,*}$ is the stoichiometry coefficients of benthic algae for the respective constituents (mg P mg^{-1} benthic algae; mg N mg^{-1} benthic algae; and (mg O_2 sec^{-1}) (mg benthic algae $sec^{-1})^{-1}$). α_B is the proportion of ammonia nitrogen available for uptake by benthic algae considering the preference for ammonia over nitrate. R is the hydraulic radius (m). Other variables are as defined above. As can be seen in 15, only growth is considered to affect nutrient concentrations; algal respiration does not play a role. Algal growth also produces oxygen.

Since the *Cladophora* model only considers phosphorus uptake, its only water column interaction is described as follows (Canale and Auer, 1982e):

$$V\frac{dP}{dt} = -\rho XA. \tag{16}$$

Equation 16 considers the time rate of change in phosphorus concentration (P; $\mu g\ P\ L^{-1}$) to be a decreasing function of the phosphorus uptake rate and the mass of *Cladophora* present (XA; $(g\ m^{-2})*m^{-2}$). V is the water column volume. A unit conversion factor is also needed for mass.

MODELING PERILITHIC ALGAE

The following sections examine the results from studies of biofilm kinetics, especially those that can elucidate the functioning of a biofilm perilithic algae. Much work has been done on this, particularly under steady-state conditions. The work has gained impetus from the widespread nature of biofilms. They occur in a wide variety of environments, from industrial processes to pristine streams. Most significant work has been done for biochemical reactors used in industrial processes. However, much of the basic theory is applicable to natural aquatic systems. It is this that the following review focuses on. Figure 1 illustrates important physical features of a biofilm. These include attachment to a solid substrate, the biofilm thickness, denoted by L, the overlying water, and an air-water interface.

BIOFILM GROWTH AND SUBSTRATE UTILIZATION

According to Atkinson (1974), the steady-state equation for constituent removal by a biofilm is given by the following

$$D_e\frac{\partial^2 C}{\partial z^2} - \frac{a\alpha C}{\beta + C} = 0, \tag{17}$$

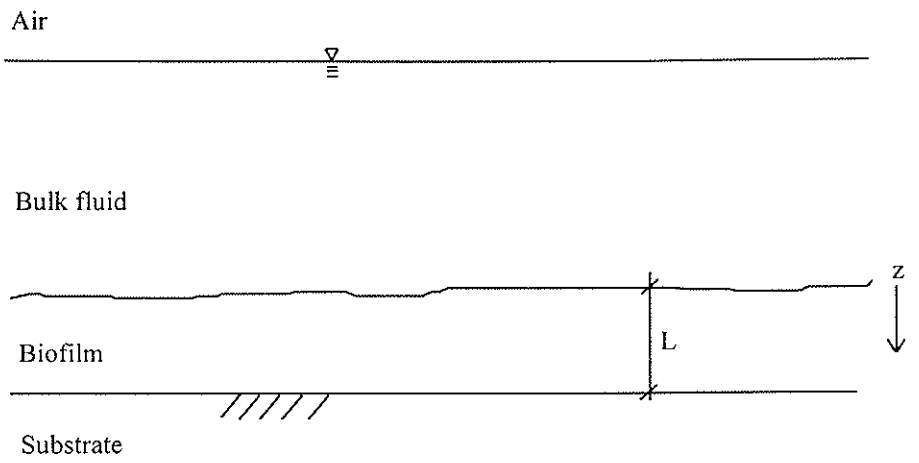

Figure 1: Diagrammatic view of a biofilm showing important physical features: its attachment to a solid substrate, the thickness of the biofilm (L), the bulk fluid overlying the biofilm, and an air-water interface.

with boundary conditions

$$z=L \qquad \frac{dC}{dz} = 0 \text{ and}$$

$$z=0 \qquad C=C^*$$

Here D_e = effective molecular diffusion coefficient within the biofilm ($mm^2\ s^{-1}$), C = constituent concentration within the biofilm ($mg\ L^{-1}$), a = area of viable organisms per biofilm volume, α and β = coefficients. L = biofilm thickness (mm), and C^* = constituent concentration at the biofilm-bulk fluid interface ($mg\ L^{-1}$). Since the biofilm is attached to a solid boundary, at depth z=L there is no gradient; the only point for exchange is the surface where z=0. Equation 17 describes the constituent's diffusion through and non-linear decay within the biofilm. It assumes there is no advective flux of nutrient through the biofilm, that molecular diffusion is constant throughout the biofilm, that the reaction kinetics of the nutrient can be described by a Monod relation, and that biofilm thickness is constant.

The solution of equation 17 would take the form

$$C=g(z,D_e,a\alpha,\beta,L,C^*) \tag{18}$$

(Atkinson, 1974). However, the opinion is expressed by Atkinson (1974) that a solution in terms of flux (N) with the bulk fluid may be more convenient. In this case the solution at z=0 is of the following form:

$$N = -D_e \frac{dC}{dz} = g\left(D_e, a\alpha, \beta, L, C^*\right). \tag{19}$$

A solution of this form is not concerned with concentration profiles within the biofilm.

A transient-biofilm model is developed by Rittman and Brunner (1984). The transient condition is the change in biofilm biomass. They consider five processes: flux through a diffusion layer; substrate utilization and transport; and biomass growth and loss. The equation

$$J = -D\frac{dC}{dz} = D\frac{C - C_s}{L_{DL}} \tag{20}$$

describes the restriction to mass transport by diffusion layer in the bulk fluid and immediately adjacent to the biofilm's surface. J = constituent flux through the diffusion layer (g m^{-2} s^{-1}); D = constituent diffusion coefficient in water (mm^2 s^{-1}); C = constituent concentration in the bulk fluid (mg L^{-1}); z = coordinate normal to biofilm surface (mm); C_s = constituent concentration at the biofilm surface (mg L^{-1}); and L_{DL} = thickness of the diffusion layer (mm).

Constituent utilization and diffusion transport within the biofilm are described by the following equation:

$$D_f\frac{\partial^2 C_f}{\partial z^2} = \frac{kX_f C_f}{K_c + C_f}. \tag{21}$$

Here D_f = molecular diffusion coefficient within the biofilm; C_f = constituent concentration within the biofilm (mg L^{-1}); k = maximum specific utilization rate of the constituent (g g^{-1} s^{-1}); X_f = biofilm density (g m^{-3}), and K_c = half-saturation constant for the constituent. This is the same as described above by equation 17.

Biofilm growth and loss at a point within the biofilm is expressed by the following equation:

$$\frac{dX_f}{dt} = Y\frac{kX_f C_f}{K_c + C_f} - b'X_f, \tag{22}$$

with Y = yield coefficient (g g^{-1}) and b' = biomass loss coefficient (s^{-1}). Biomass loss is accounted for by decay and shear losses. (It is reasonable to assume that shear losses occur from the surface downwards into the biofilm, while decay occurs throughout the biofilm depth.)

Equation 22 is for one microbial type (species), however other research has included more than one species and their interaction in the biofilm. A numerical simulation of a mixed-culture biofilm was done by Kissel, McCarty, and Street (1984). They developed a dynamic, finite-element model composed of four types of bacteria and their decay products. The bacteria include aerobic and facultative anaerobic heterotrophs and the

nitrifying bacteria, *Nitrosomonas* and *Nitrobacter*. Five different substrates could be utilized by these bacteria: oxygen, benzoate, ammonia-nitrogen, nitrite-nitrogen, and nitrate-nitrogen.

The growth of live biomass for each bacterial type was governed by the following non-dimensional equation

$$\frac{dX^*_{A,j}}{dt^*} = [\tau kY]M_G X^*_{A,j} - [\tau b]M_D X^*_{A,j}, \text{ and} \tag{23}$$

the growth of inert mass from biomass decay was described by the following equation

$$\frac{dX^*_{I,j}}{dt} = \left[\tau(1 - f_d)b\right]M_D X^*_{A,j}. \tag{24}$$

Both equations describe mass increases at a point within the biofilm. $X^*_{A,j} = X_{A,j}/X_{total}$, $X_{A,j}$ = active biomass of jth bacterial type (mg L^{-1}), X_{total} = total biomass of all bacterial types (mg L^{-1}), $t^* = t/\tau$, τ = characteristic time of the system, k = maximum growth rate (g substrate g^{-1} cells day^{-1}), Y = yield coefficient (g cells g^{-1} substrate), M_G = Monod term for growth, b = decay rate (day^{-1}), M_D = Monod term for decay, $X^*_{I,j} = X_{I,j}/X_{total}$, $X_{I,j}$ = inert mass derived from decay of jth bacterial type (mg L^{-1}), and f_d = degradable cell fraction. The Monod relation for growth could be selected as either a minimum of, or the product of, two substrates, one of which is an electron donor (benzoate, ammonia, or nitrite) and the other an electron acceptor (oxygen, nitrite, or nitrate). The biofilm density was assumed constant throughout the depth. Equations were constructed for both aerobic and anaerobic conditions.

Since Kissel, McCarty, and Street (1984) were solving for five substrates under both aerobic and anaerobic states. Ten equations were necessary for this; they will not be described here, except that they take the general form

$$\frac{\partial S^*_i}{\partial t^*} = \left[\frac{\tau D_{f,i}}{L_c^2}\right]\frac{\partial^2 S^*_i}{\partial z^{*2}} - R^*_i, \tag{25}$$

where $S^*_i = S_i/K_{S,i}$, or S_i/C_s for oxygen, S_i = ith substrate concentration (mg L^{-1}), $K_{S,i}$ = ith half-saturation coefficient, $D_{f,i}$ = diffusion of ith substrate in biofilm (mm^2 day^{-1}), L_c = a characteristic length of the system, $z^* = z/L_c$, z = depth (mm), and R^*_i = sources and sinks of ith substrate.

They examined the characteristic times of the system and concluded it was appropriate to solve the substrate transport equations for the steady-state; since in comparison to biomass growth times these were 10^1 to 10^4 times faster.

BIOFILM DETACHMENT

Using data reported by Trulear and Characklis (1980), Rittman (1982) derived a biofilm loss rate coefficient based on fluid shear stress. The data were collected from annular biofilm reactors where the inner annuli were rotated at various rates. After converting the rotational rate to shear stress the following relations were obtained:

$$\frac{dX_f L_f}{dt} = -b' X_f L_f, \text{ where} \tag{26}$$

$$b' = b + 0.0842\left(\frac{\tau}{1 + 443.2(L_f - 0.003)}\right)^{0.58} \quad \text{for } L_f > 30\mu m \text{ and} \tag{27}$$

$$b' = b + 0.0842\tau^{0.58} \quad \text{for } L_f \leq 30\mu m. \tag{28}$$

where X_f = biofilm density (mg cm^3), L_f = biofilm thickness (cm), b = biomass decay coefficient (day^{-1}), and τ = shear stress (dyne cm^2). The coefficient b′ is a combination of decay and shear losses. Note that in regard to X_f, equation 26 is linear, but in regard to L_f it is non-linear.

Bakke, *et al* (1990) proposed that biofilm detachment follows a shear stress function of the following form:

$$r_{e,X} = k^*_{e,X} \tau X_f, \text{ where} \tag{29}$$

$$\tau = 0.04\left(\frac{d}{\nu}\right)^{-0.25} \rho^{0.75} v^{1.75}. \tag{30}$$

$r_{e,X}$ = erosion rate per unit area of biofilm (g cm^{-2} s^{-1}), $k^*_{e,X}$ = shear-related erosion rate coefficient (mm s^{-1}), τ = shear stress on the biofilm surface of a pipe (gm mm^{-1} s^{-2}), X_f = biofilm density (gm cm^{-3}), d = diameter of a pipe (cm), ν = kinematic viscosity ($m^{-2}s^{-1}$), ρ = water density (gm cm^{-3}), and v = fluid velocity (cm s^{-1}). Since this was derived for fluid flow in ducts, it is not appropriate in its current form for application to open-channel flow.

A general model for biofilm detachment has been proposed by Stewart (1993). It relates the mass of material lost and a coefficient to the loss rate. The coefficient can be a function of biofilm thickness, shear stress, physiological state of the biofilm, et cetera. The model equation is a follows:

$$r_d = F_d(L_f - z_d)A_d X_f, \tag{31}$$

where r_d = rate of biofilm detachment (g mm^{-2} s^{-1}), X_f = biofilm density (gm cm^{-3}), L_f = biofilm thickness (mm), F_d = detachment frequency for the whole biofilm thickness (s^{-1} mm^{-2}), z_d = biofilm thickness remaining after detachment (mm), and A_d = area of detachment (mm^2). Note that the term $(L_f - z_d)A_d X_f$ is the mass of the detached particle. The detachment frequency and biofilm density could vary over the biofilm depth, such that

$$r_d = \int_0^{L_f} f_d(z)(L_f - z)A_d X_f(z)dz, \text{ and} \tag{32}$$

$$F_d = \int_0^{L_f} f_d(z)dz. \tag{33}$$

Here $f_d(z)$ = the detachment frequency at a point in the biofilm (s^{-1} mm^{-3}). Pertinant physical features for equation 32 are defined in the figure 2.

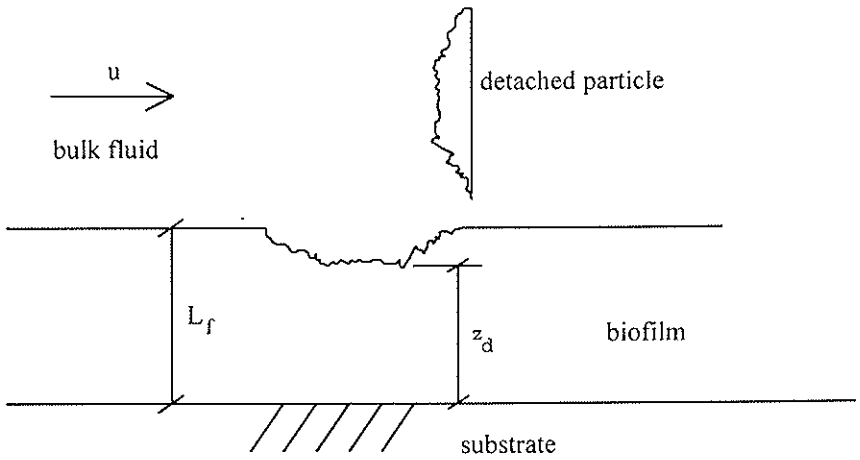

Figure 2: Biofilm detachment definition diagram adapted from Stewart (1993). It shows the detachment of a particle from the biofilm at an distance L_f-z_d below the surface.

Various forms of $f_d(z)$ were proposed. If $f_d(z)$ were constant throughout the biofilm depth, it takes the following form:

$$f_d(z) = \frac{k_d}{A_d}, \tag{34}$$

which gives the following result, when substituted into equation 32:

$$r_d = \tfrac{1}{2} k_d X_f L_f^2. \tag{35}$$

In equations 34 and 35, k_d = detachment rate coefficient (g mm^{-1} s^{-1}). If $f_d(z)$ occurs at a preferred location (z_d), it takes the following form:

$$f_d(z) = \frac{k_d \delta(z - z_d)}{A_d}, \tag{36}$$

then when substituted into equation 32, the following result is produced:

$$r_d = k_d X_f (L_f - z_d). \tag{37}$$

For equations 36 and 37, k_d = detachment rate coefficient (g s^{-1}). Finally, if $f_d(z)$ is a function dependent on the local growth rate ($\mu(z)$), then the following form results:

$$f_d(z) = \frac{k_{d1}\mu(z) + k_{d2}}{A_d}. \tag{38}$$

Integrating, as described in equation 32, gives the following result:

$$r_d = k_{d1} X_f \int_0^{L_f} \mu(z)(L_f - z)dz + \tfrac{1}{2} k_{d2} X_f L_f^2. \tag{39}$$

For equations 38 and 39, k_{d1} = growth related detachment rate coefficient (dimensionless), k_{d2} = constant detachment rate coefficient (g mm^{-1} s^{-1}), and $\mu(z)$ = growth rate at a point in the biofilm (day^{-1}).

EXPERIMENTAL METHODS

Any water quality modeling exercise requires estimates of the rate coefficients and parameters used in the differential equations. For benthic algae, the rate coefficients include maximum specific growth rate, respiration rate, mortality, and scour rate. With the exception of scour rate, a range of values for each these rates is available in Bowie, *et al* (1985).

For filamentous algae, scour rate is a function of the drag force and tensile strength of the filament. The filament is free-streaming in the fluid medium. However, it is attached to cobble surfaces and the portion near the point of attachment streams in the region of flow separation, which reduces the velocity but increases the turbulence. If the filament is long enough, the portion downstream of the separation zone is subjected to higher velocity. Drag force is determined by the shape and length of the alga and the fluid velocity in the neighborhood of the filament. Tensile strength is a function of the thickness of the filament and its age. As discussed above, Canale and Auer (1982e) conducted experiments for estimating scour rate of *Cladophora* and derived an empirical relation of wind speed to scour rate. They also stated that further work was needed on this subject. Grenney and Kraszewski (1981) also state that further research is needed on scour of benthic algae. Detachment of biofilms in general and algal biofilms in particular are not well understood (Stewart 1993).. Laboratory tests on bacterial film detachment have been done, but there is no agreement on the mechanisms of detachment, nor their mathematical description. While this is an important feature of biofilm growth, it is beyond the scope of this study to evaluate this issue; it relies on descriptions of detachment found in the literature.

Estimates of benthic algae biomass in the natural water body, for both attached filamentous algae and perilithic biofilm, along with nutrient and other environmental factors that influence growth rates, are needed for calibration. The following sections discuss methods used in measuring scour rate estimates and biomass.

ATTACHED FILAMENTOUS ALGAE

Biomass measurements were collected for calibration purposes. Flume studies have also been conducted to derive scouring rate estimates.

BIOMASS ESTIMATES

In-stream sampling at several points along the length of the Russian River was done to provide biomass estimates for calibration. Sampling occurred over the growing season while the sample sites were accessible from the shore; flood flows restricted access to the bed for harvesting benthic algae. Figure 3 shows the sampling site locations for *Cladaphora* at Monte Rio, Johnson's Beach, Midway Beach, and Odd Fellows. These sites were known locations where *Cladaphora* occurred and were established sampling sites of the North Coastal Regional Water Quality Control Board.

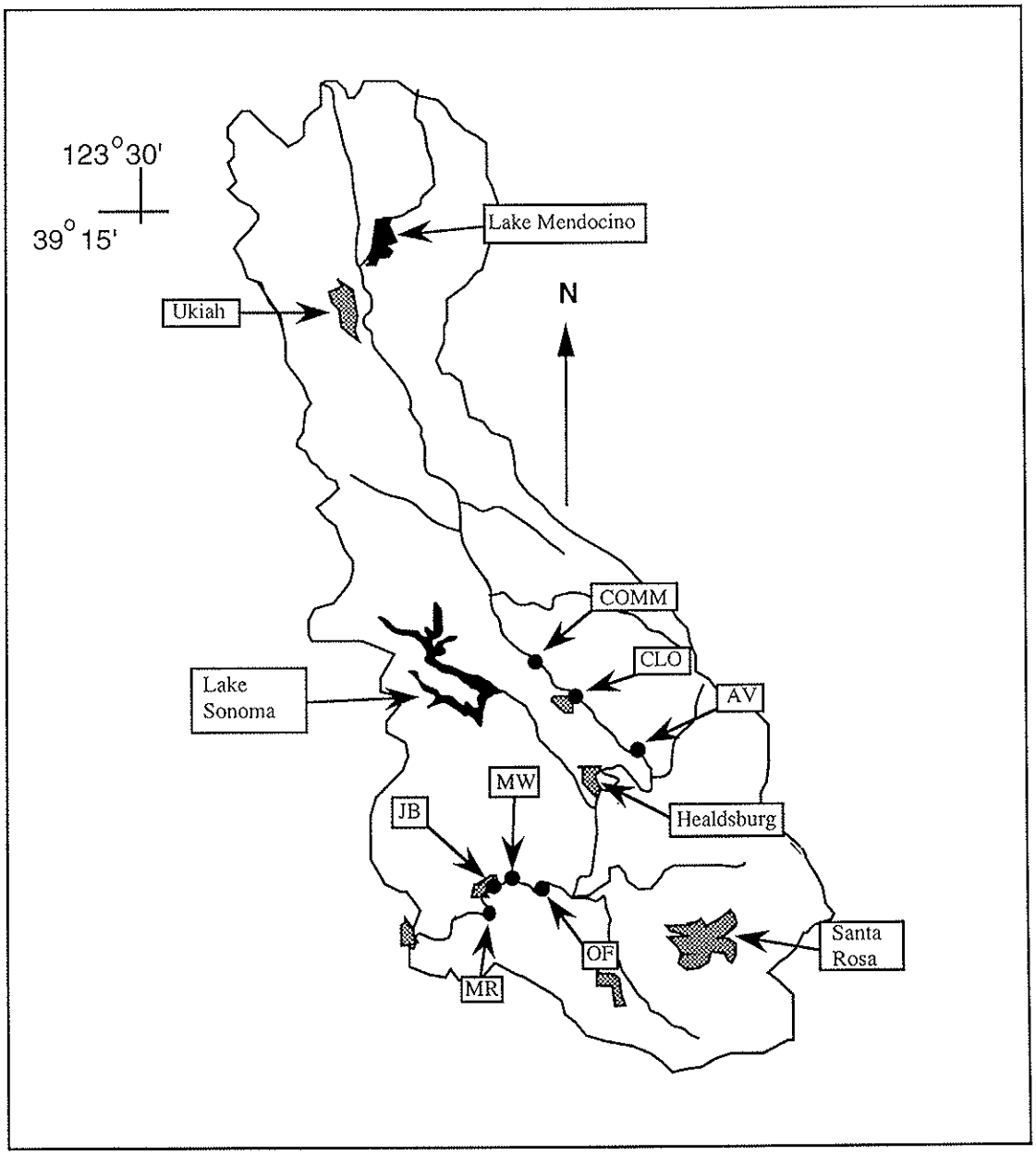

Figure 3: Map of Russian River basin and benthic algae sampling locations. Filamentous algae sampling sites are Monte Rio (MR), Johnson's Beach (JB), Midway Beach (MW), and Odd Fellows (OF). Perilithic biofilm sampling sites are Commuski Station (COMM), Cloverdale (CLO), and Alexander Valley (AV). River kilometers 9.4 is located below MR, and river kilometer 26.6 is in the neighborhood of OF.

At these sites, filamentous algae were not continuously distributed over the wetted perimeter, so the mean biomass density was estimated by sampling at four evenly spaced locations in the cross-section. At each location an area of 0.437 m^2 was sampled within a circular hoop. All filamentous algae and their holdfasts present in that region were harvested.

After biomass within each hoop was collected, the samples were rinsed to remove sand and other extraneous material. The dry weight of each hoop mass was determined after drying at 105 °C.

DETACHMENT EXPERIMENTS - FLUME STUDY

The general equation of filamentous algal growth is

$$\frac{d(A_b B_{afa})}{dt} = (\mu_{net} - g)A_b B_{afa} - d_{afa}, \tag{40}$$

where B_{afa} = attached filamentous algae density (gm m^{-2}), A_b = bed area at point of solution (m^2), μ_{net} = net growth rate after considering growth, respiration, and mortality (day^{-1}), g = grazing losses (day^{-1}), and d_{afa} = mass flux loss due to detachment (gm day^{-1}).

A dimensional analysis of pertinent variables is a useful way for analyzing the experimental results. Relevant variables include $\dot{m}_{ba}$ = mass loss rate from attached algae (gm day^{-1}), m_{ba} = mass of attached algae (gm), u = velocity near the attached algae mass (m s^{-1}), ρ_w = water density (gm cm^{-3}), d = water depth (m), and Re = Reynolds number. The analysis gives the following result

$$\dot{m}_{ba} = u\rho_w d^2 \, f\left(Re, \frac{m_{ba}}{\rho_w d^3}\right). \tag{41}$$

While length of the individual filaments may be a relevant parameter, the variability of filament lengths observed in the field would make its inclusion problematic. Examination of the data for the nondimensional variables in the function when compared with the mass loss rate and with each other gives the structure of the function.

The flume studies were designed to estimate mass flux due to detachment using filamentous algae collected from the field. Samples of filamentous algae which were attached to substrate (cobble) were brought to the laboratory. These were collected from the Russian River and carried in buckets of river water. Laboratory tests began within three hours of collection. The cobbles with attached algae were laid within a bed of cobble placed on the flume bed. The cobbles were prevented from moving by sitting on a six foot long aluminum sheet with a half inch lip at the downstream end.

Biomass flux was measured as follows: (1) set up wire fencing trap downstream at location to prevent backwater effects; (2) place acoustic Doppler velocity probe at a depth

to measure the velocity near the bed, (3) start the pump, (4)sample the trap at frequent intervals to reduce likelihood of loss of catch; (5) continue until a sufficient mass has detached, but not so much as to significantly reduce the biomass from which detachment is occurring; and (6) when the run is complete, collect the entire mass of attached algae remaining. The sum of the remaining biomass and total measured loss is the total initial biomass. Figure 4 illustrates the components of the procedure.

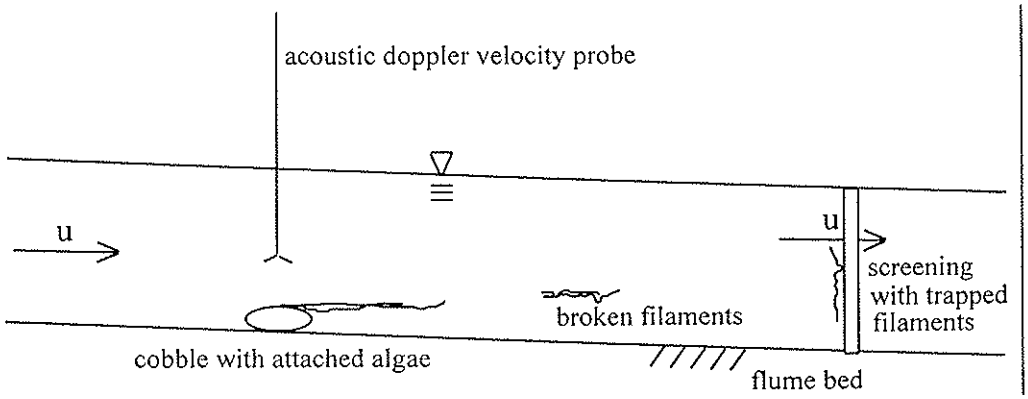

Figure 4: Flume setup for measuring scour rate of filamentous algae. The cobbles with attached algae are imbedded within other cobble (not shown) of similar size.

PERILITHIC ALGAE - BIOMASS ESTIMATES

Perilithic algae occur as films on the bed of water bodies. Associated with those films are other micro- and macro-organisms which will contribute to its thickness, depending on nutrient loading (inorganic and organic). For the purpose of this study, it will be assumed that one algal species is present to account for autotrophic production in the biofilm. Further, it is assumed that algal growth dominates the biofilm, but that bacterial degradation of soluble organics within the biofilm is occurring in conjunction with algal growth. Hence, the focus for biomass estimates will be on chlorophyll *a*, dry weight, and ash-free dry weight.

Biomass contributed by attached microscopic algae is more difficult to collect and quantify than attached filamentous algae. Typically, some artificial substrate is placed in the water column and algae are allowed to grow over an extended period, typically weeks or months, before harvesting. Wetzel (1975) states this approach fails to account for biological and hydrodynamic influences, but that it may be suitable for examination of attached algae accumulation rates (net growth rates). He suggests that further research on methods for estimating is needed, particularly without resorting to the use of artificial substrates.

The method used for collecting biomass samples was derived from Corning, *et al* (1989). The sampling sites on the Russian River are seen in figure 3 as Commusky Station, Cloverdale, and Alexander Valley. As for the attached filamentous algae these were established sampling sites of the North Coastal Regional Water Quality Control Board.

Rock samples were collected from the river site. Using a soft bristled brush, the upper surface of rock was scraped and rinsed with deionized water. Care was taken to prevent rinsing of surfaces not scraped. The rinsate was collected in a 500 ml graduated cylinder and the total volume of rinse water measured. The collection area on the rock surface was measured by laying aluminum foil over the upper surface and trimming the edges to match the area scraped. Any folds were also trimmed. To compute the area, the weight of foil was multiplied by the area per unit weight factor for the foil. This process is repeated on several other rocks collected from the site until a sufficient sample size has been collected. This was dictated by the sample volumes needed for chlorophyll a, gravimetric, and settling tests. Samples were stored on ice until processed.

Sample processing began by thorough mixing and subsampling. The subsamples were measured for dry weight, ash-free dry weight, settling volume, and chlorophyll *a* content. Dry weights were determined by procedures listed in Standard Methods (APHA, 1985). Chlorophyll *a* samples were submitted to a private laboratory for analysis. Settling volumes were measured using an Imhoff cone according to Standard Methods (APHA, 1985). It gives an indication of the total bulk volume and hence the thickness of the biofilm. The thickness is computed by the total volume of collected biofilm over the area collected.

EXPERIMENTAL RESULTS

BIOMASS - ATTACHED FILAMENTOUS AND PERILITHIC

Tables 1 and 2 give the results of field biomass measurements for the Russian River. The collection period was during May, 1994. Two collection periods (5/9/94 and 5/11/94) corresponded with water quality sampling conducted by the North Coastal Regional Water Quality Control Board.

The peak filamentous algae biomass was 40 gm/m^2 on 5/4/94 at the Midway beach site, approximately 1 mile above Guerneville, CA. Other sites had lesser biomass and by 5/19/94 the Odd Fellows site had essentially no filamentous algae remaining. The Midway site was inundated after 5/11/94 by backwater from the recreation dam at Guerneville. For comparison, the maximum biomass seen by Grenney and Kraszewski. (1981) was on the order of 100 gm/m^2.

The dry weight densities for the perilithic biofilm were of the same magnitude at seen for the attached filamentous (Table 1). Since the biofilm is a heterogeneous mixture of living and inert material, the chlorophyll *a* content is useful for estimating the algal biomass. However, for the filamentous algae the whole collected mass is algae, so that the dry weight biomass is the appropriate estimate and chlorophyll *a* is not needed. At two stations (CLV and AV) dry weight and chlorophyll *a* decreased between 5/9/94 and 5/25/94, while at one station (COMM) all measured values increased. Particularly noteworthy was the large thickness (3000 μm) estimate for AV on 5/9/94 and subsequent loss of the biofilm (thickness 200 μm) by 5/25/94. This was visually apparent, since at

the earlier date there was a distinct gelatinous film on the cobble, which was not apparent later.

Table 1: Attached filamentous algae results for the Russian River, CA. The stations correspond to the following river mile locations: OF (Odd Fellows) ; MW (Midway) ; JB (Johnson's Beach) ; and MR (Monte Rio) .

Date	Station	(gm/m^2) wet weight	dry weight
5/4/94	OF	114	20
	MW	266	44
5/11/94	OF	110	22
	JB	136	26
	MR	153	25
5/19/94	OF	0	0

Table 2: Perilithic biofilm results for the Russian River, CA. The stations correspond to the following river mile locations: COMM (Commusky Station) ; CLV (Cloverdate) ; and AV (Alexander Valley).

Date	Station	(gm/m^2) dry weight	ash-free weight	chlorophyll *a*	(μm) Biofilm Thickness
5/9/94	COMM	28.0	4.2	0.041	300
	CLV	24.8	4.4	0.043	300
	AV	28.4	13.7	0.125	3000
5/25/94	COMM	58.1	37.6	0.051	600
	CLV	12.4	4.6	0.003	400
	AV	12.9	9.6	0.017	200

FLUME STUDY RESULTS

Dimensional analysis was used to examine the flume study results. This procedure places pertinent variables in non-dimensional form in order to compare relationships between them. These non-dimensional variables are called pis (π_n). π_1 is the ratio of detached biomass flux, the ultimate variable of interest, to fluid flux. π_2 is the ratio of attached biomass to fluid mass. π_3 is the Reynolds number. While six separate tests were made, only four had velocity measurements near the cobble bed surface. Plots of the results suggest a strong relation between the Reynolds # and mass flux (π_1). This is expected, since the detachment mechanism is thought to function through the drag force on attached filaments. Many tests are required for a rigorous analysis; hence, it is planned that more tests will be performed when more attached growth data are available.

Table 3: Nondimensional variable values obtained from flume experiments to detach filamentous algae under various velocity regimes.

Run #	π_1 (Ratio of detached biomass flux to fluid flux)	π_2 (Ratio of biomass to fluid mass)	π_3 (Reynolds Number)
1a	1.18×10^{-9}	0.00331	18300
1b	2.03×10^{-10}	0.00328	14800
2	2.16×10^{-10}	0.00252	14100
3		0.00235	
4a	3.22×10^{-9}	0.00363	22900
4b		0.00355	

DEVELOPMENT OF MODEL EQUATIONS

For the present purpose, benthic algae are classified based on the algal "form" and the "route" by which nutrients are accessed. Form is intended to indicate whether the organism is free-streaming in the turbulent region of fluid flow, especially applicable to 1D systems, or whether the organisms form a film on solid surfaces lining the bed. The former describes filamentous algae, while the latter is considered as a perilithic biofilm dominated by diatomaceous algae. In the case of the Russian River, the site of application, the filamentous algae of concern is *Cladophora.*

For filamentous algae, the transport of nutrients to the organism is not of concern in a 1D system, since the water column in which the organisms grow is considered to be completely mixed and no diffusion process is necessary to transport nutrient from the water column to the algal surface. A vertically averaged 2D system assumes complete mixing in the vertical direction (non-stratified flows), and transport from a source is accomplished through the transport equations, as for the 1D system. In a horizontally averaged, 2D system, the nutrient transport is also accomplished by the water column transport equations, but vertical stratification is allowed. In both 2D systems the assumption of no diffusion process is made; the same as used for the 1D system.

A perilithic algal biofilm is assumed to lie within a laminar sublayer in 1D and 2D systems. No advective fluid flow is assumed to occur within the film. Hence, nutrient transport occurs from diffusion, which means algal growth within the biofilm is limited by the diffusion rate. Also, within the laminar sublayer, nutrient transport to the biofilm surface from the turbulent region occurs by diffusion, since laminar flow implies no fluid mixing across streamlines.

The development of the model equations reflects these considerations of the algal growth forms and nutrient transport route. The development of the filamentous algae and perilithic algae biofilm equations are presented below.

Note: Variable definitions and units are listed at the end of the report in Appendix A.

ATTACHED FILAMENTOUS ALGAE

Attached filamentous algae are, as the name implies, fixed to a waterbody's bed. Unlike planktonic (suspended) algae it is not subject to advective transport by fluid motion; however, it is subject to detachment. Tracking this detached biomass would necessitate inclusion of advective processes, but the original biomass is not subject to advection. Thus attached filamentous algae growth can be mathematically described at a point on the bed of the water body with an ordinary differential equation. It includes terms for net growth from internal processes in response to the nutrient regime ($\mu_{net(t)}$; day^{-1}), a term for grazing losses by aquatic invertebrates and fish ($g_{(t)}$; day^{-1}), and for hydrodynamic detachment ($d_{(t)}$; gm day^{-1}).

$$\frac{d(A_b B_{afa})}{dt} = (\mu_{net\,(t)} - g_{(t)}) A_b B_{afa} - d_{afa\,(t)} \qquad (42a)$$

where B_{afa} = average biomass density of attached filamentous algae over whole bed area (gm m^{-2}), A_b = total bed area of the water body (for 1D streams this is the wetted perimeter) (m^2), and d_{afa} = detachment flux caused by drag on the filaments from fluid flow (gm day^{-1}). The product of A_bB_{afa} is the total mass of attached filamentous algae (M_{afa}). Instead of expanding the LHS derivative and directly solving for density, the mass (A_bB_{afa}) can be solved first, then the biomass density obtained by dividing the mass by the bed area. For a vertically averaged 2D system, the depth component (z) is eliminated, giving a system that inherently includes the surface area (x and y components). In this case A_b is equal to unity, and the biomass density is equal to the biomass itself.

Equation 42a is solved using a 2nd order Runge-Kutta (modified Euler) method, with the terms which are function of time evaluated at the beginning and end of the time step. Higher order methods are not suitable, since concentrations used to evaluate $\mu_{net(t)}$ and other time related terms are not available from the transport equation solution. It provides concentration results only at the beginning and end of each time step, as well.

The net growth rate ($\mu_{net(t)}$) is given by the following

$$\mu_{net} = \mu_{max} F_L \min(F_P, F_N) F_H - \rho - m \qquad (42b)$$

with μ_{max} = maximum specific growth rate for the filamentous algal species (day^{-1}); $F_L = \frac{I}{K_L+I}$; I = the light intensity at the bed (langleys); K_L = half-saturation constant for light (langleys); $F_P = \frac{P}{K_P+P}$; P = dissolved orthophosphate concentration near the filamentous algae (mg L^{-1}); K_P = half-saturation coefficient for phosphorus (mg L^{-1}); $F_N = \frac{N}{K_N+N}$; N = inorganic nitrogen (nitrate and ammonia) concentration near the filamentous algae (mg L^{-1}); K_N = half-saturation coefficient for nitrogen (mg L^{-1}); $F_H = 1 - B_{hd}/B_{max}$; $B_{hd} = M_{afa}/A_h$; A_h = area of habitat available for growth; B_{max} = maximum biomass density that can be support by the habitat given optimal growing conditions; ρ = algal respiration rate (day^{-1}); and m = algal mortality (day^{-1}). The available habitat suitable for growth is typically hard substrate (gravel, cobble, bedrock, etc.) that is not readily removed by bed erosion.

BIOFILM

Biofilms in natural systems are heterogeneous systems composed of inert, organic and inorganic materials and several possible types of active biomass (algae, bacteria, fungi, etc.)., These will have distributions through the biofilm that are functions of nutrient and oxygen concentrations in the biofilm, light penetration, and history of exposure to nutrients and suspended sediment in the water column.

The density of solid matter is such that it is a significant fraction of a control volume, creating a void space that is filled with water. This is particularly important when considering the concentration of nutrient available; an active organism will "see" the concentration in the fluid, not that averaged over the whole control volume. Schematically, one can partition the

control volume into different volume fractions. The product of the volume fraction concentration by its volume fraction gives the average control volume concentration.

BIOFILM GROWTH EQUATIONS

Figure 5 is a definition sketch from which the mass balance equations for biofilm growth are derived. The general growth equation is described as the accumulation of mass as a function of the change in mass in the control volume and the net mass flux through the control volume. An important assumption is that average mass density (X_f) remains constant throughout the biofilm and control volume, but the fraction of the mass type (f_k) can change. This implies the solid's density is also constant. This necessitates that at least two types of mass be present. This, however, does not present a problem; since, as stated above, biofilms are heterogeneous systems. The following mass balance equation for biofilm growth reflects these assumptions, with the index k indicating the different types of materials present.

$$\frac{d(1-n)(f_k)}{dt} C_S A \Delta z = (\text{growth})_k + (\text{influx})_k - (\text{efflux})_k \qquad (43)$$

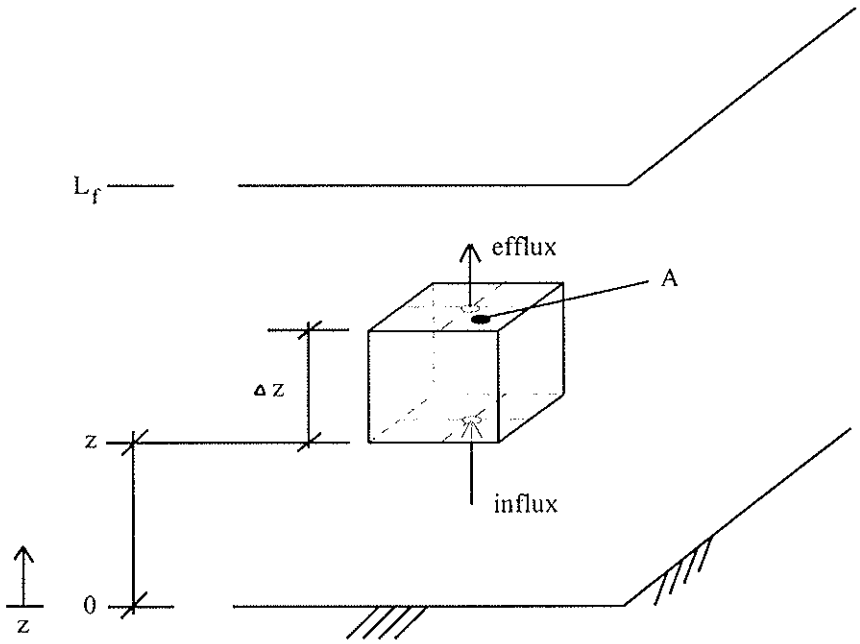

Figure 5: Definition diagram for biofilm growth model equations. A control volume located between a solid substrate (z = 0) and the biofilm surface (z = L_f) has a length (Δz) and a surface area (A). Mass flux of biomass occurs through the control volume as a result of growth of active and inert biomass.

The volume fraction, n, is needed to account for void space present in the biofilm, which is occupied by fluid, and for the current case, it is considered to be constant. As a result equation 43 becomes

$$(1-n)\frac{d(f_k)}{dt}C_S A\Delta z = (\text{growth})_k + (\text{influx})_k - (\text{efflux})_k \qquad (44)$$

Considering only algal growth and the accumulation of inert material from insoluble respiration and mortality products, the growth rate terms for the control volume are as follows:

$$(\text{growth rate})_1 = (\mu_1 - \rho_1 - m_1)(1-n)f_1 C_S A\Delta z \qquad (45)$$

$$(\text{growth rate})_3 = m_1(1-f_d)(1-n)f_1 C_S A\Delta z \qquad (46)$$

where

$$\mu_1 = \mu_{1,max} F_L \min\{F_P, F_N, F_{Si}\} \quad \text{and} \qquad (47)$$

$$F_* = \frac{C_*}{K_* + C_*}. \qquad (48)$$

Note that μ_1 is a function of depth (z); since it is determined by the nutrient concentrations which vary with z. ρ_1 and m_1 are typically regarded as constants in water quality models[1]. Equation 46 presumes only mortality (m_1) contributes to inert, particulate, organic matter, while ρ_1 enters the liquid phase as soluble organic matter.

Figure 6 illustrates the result of a constant density biofilm. The growth from each control volume advects to keep the total mass density constant. It results in the flux of mass (active and inert) away from the surface of attachment. Each control volume contributes to mass flux, so that the further a control volume is from the attachment surface, the greater the flux. The following discrete equation states this in a formal manner and is equal to the total mass flux across the nth control volumes' upper face.

$$\begin{aligned} \text{flux}\big|_n &= (1-n)C_S A V_{n,i} \\ &\sum_{i=1}^{n}(\mu_1 - \rho_1 - m_1)_i (1-n)(f_1)_i C_S A\Delta z \\ &+ \sum_{i=1}^{n} m_1(1-f_d)(1-n)(f_1)_i C_S A\Delta z \end{aligned} \qquad (49)$$

where

[1] However, it is possible there may be some dependency of ρ_1 on μ_1. This can be thought of as reflecting the "leakiness" of algal cells during growth. See Haack and McFeters (1982).

$$V_n = \sum_{i=1}^{n}(\mu_1 - \rho_1 - m_1)_i (f_1)_i \Delta z + \sum_{i=1}^{n} m_1(1-f_d)(f_1)_i \Delta z \quad (50)$$

The velocity (V_n) is a function of the growth rates occurring in the biofilm at depth. Assuming growth varies in a continuous manner through the biofilm, one can integrate over the biofilm depth 0 to z, to obtain the total flux:

$$\text{flux}|_z = (1-n)C_S A V_{(z)} = \int_0^z (\mu_{1(\zeta)} - \rho_1 - m_1)(1-n) f_{1(\zeta)} C_S A d\zeta + \int_0^z m_1(1-f_d)(1-n) f_{1(\zeta)} C_S A d\zeta \quad (51)$$

where

$$V_{(z)} = \int_0^z (\mu_{1(\zeta)} - \rho_1 - m_1) f_{1(\zeta)} d\zeta + \int_0^z m_1(1-f_d) f_{1(\zeta)} d\zeta = \int_0^z \{\mu_{1(\zeta)} - \rho_1 - m_1 f_d\} f_{1(\zeta)} d\zeta \quad (52)$$

Note, that ζ is a dummy variable for biofilm depth. As can be seen, growth through the biofilm from 0 to z is regarded as a velocity. The term $X_f A$ can be removed from the integral since it is constant. Re-arranging the terms yields the total flux term (fl(z)):

$$fl_{(z)} = (1-n)C_S A V_{(z)} = (1-n)C_S A \int_0^z \{\mu_{1(\zeta)} - \rho_1 - m_1 f_d\} f_{1(\zeta)} d\zeta \quad (53)$$

Dividing by $C_S A$ and changing the upper limit of integration to the biofilm surface (L_f) gives the biofilm surface velocity:

$$\frac{dL_f}{dt} = \int_0^{L_f} \{\mu_{1(z)} - \rho_1 - m_1 f_d\} f_{1(z)} dz \quad (54)$$

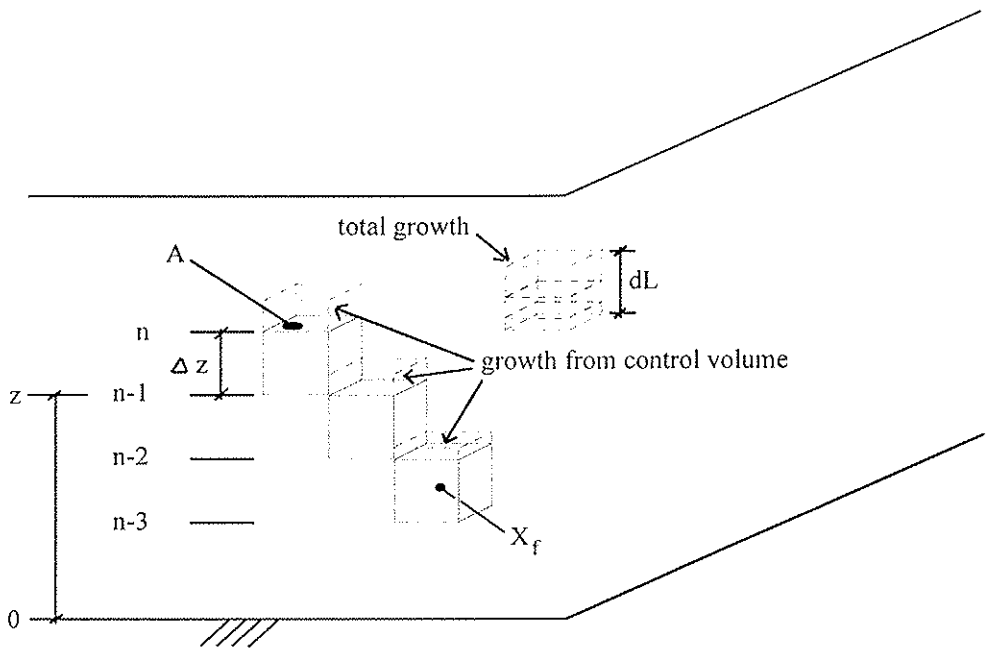

Figure 6: Illustration of physical result of assuming constant X_f. The growth in any control volume is transported away from the bed. The total growth at any location, say $z + \Delta z$, is the sum of all the growth occurring below that point. Since density is constant, an increase in length (dL) results, and the flux of material through each control volume is a function of the depth within the biofilm. Control volumes are staggered to illustrate the effect of growth in each.

The mass flux into and out of the control volume (see figure 5) for each component (i) is simply the total mass flux (equation 53) times the fraction present:

$$(\text{influx})_1 = (1-n)f_{1(z)}C_S A V_{(z)} \tag{55}$$

$$(\text{efflux})_1 = (1-n)f_{1(z+\Delta z)}C_S A V_{(z+\Delta z)} \tag{56}$$

$$(\text{influx})_3 = (1-n)f_{3(z)}fl_{(z)} \tag{57}$$

$$(\text{efflux})_3 = (1-n)f_{3(z+\Delta z)}fl_{(z+\Delta z)} \tag{58}$$

Substituting equations 55-58, and 46 into equations 43 and 44 yields the following discrete forms of the growth equations. (They are considered discrete since the velocity term is from z to z+Δz, and the growth and accumulation terms are for the control volume.)

$$(1-n)\frac{d(f_1)}{dt}C_S A\Delta z = (\mu_i - \rho_1 - m_i)(1-n)f_i C_S A\Delta z + (1-n)f_{1(z)}C_S A V_{(z)} - (1-n)f_{i(z+\Delta z)}C_S A V_{(z+\Delta z)} \tag{59}$$

$$(1-n)\frac{d(f_3)}{dt}X_f A\Delta z = m_1(1-n)(1-f_d)f_1 X_f A\Delta z + (1-n)f_{3(z)}X_f AV_{(z)} - (1-n)f_{3(z+\Delta z)}X_f AV_{(z+\Delta z)} \quad (60)$$

Dividing equations 59 and 60 by Δz and taking the limits of their flux terms, as $\Delta z \rightarrow 0$, gives the following partial result for the kth constituent:

$$\begin{aligned} &\lim_{\Delta z\to 0}\frac{-(1-n)C_S A\left\{f_{k(z+\Delta z)}V_{(z+\Delta z)} - f_{k(z)}V_{(z)}\right\}}{\Delta z} \\ &= -\lim_{\Delta z\to 0}\frac{g_{k(z+\Delta z)} \quad g_{k(z)}}{\Delta z} \\ &= -\frac{\partial(g_{k(z)})}{\partial z} \\ &= -(1-n)C_S A\frac{\partial}{\partial z}\left\{f_{k(z)}V_{(z)}\right\} \end{aligned} \quad (61)$$

Substituting the result of 61 into equations 59 and 60 and expressing all derivatives as partials gives a derivative form of the growth equations:

$$(1-n)\frac{\partial(f_{1(z)})}{\partial t}C_S A = (\mu_{1(z)} - \rho_1 - m_1)(1-n)f_{1(z)}C_S A - (1-n)C_S A\frac{\partial}{\partial z}\left\{f_{1(z)}V_{(z)}\right\} \quad (62)$$

$$(1-n)\frac{\partial(f_{3(z)})}{\partial t}C_S A = m_1(1-n)(1-f_d)f_{1(z)}C_S A - (1-n)C_S A\frac{\partial}{\partial z}\left\{f_{3(z)}V_{(z)}\right\} \quad (63)$$

The flux term of each equation is expanded using the product rule. Also since X_f, n, and A are not functions of z or t, the growth equations can be simplified to:

$$\frac{\partial(f_{1(z)})}{\partial t} = (\mu_{1(z)} - \rho_1 - m_1)f_{1(z)} - \frac{\partial(f_{1(z)})}{\partial z}V_{(z)} - f_{1(z)}^2(\mu_{1(z)} - \rho_1 - m_1 f_d) \quad (64)$$

$$\frac{\partial(f_{3(z)})}{\partial t} = m_1(1-f_d)f_{1(z)} - \frac{\partial(f_{3(z)})}{\partial z}V_{(z)} - f_{3(z)}f_{1(z)}(\mu_{1(z)} - \rho_1 - m_1 f_d) \quad (65)$$

The first terms on the right-hand-sides of 64 and 65 are growth terms; the second are flux terms considering the change in the fraction change with depth; and the third terms are fluxes considering the change in growth rate with depth.

The boundary condition is governed by the physical processes at the biofilm surface; at the attachment surface no flux of material is allowed. Material can be deposited or detached from the surface. According to Gujer and Wanner (1990), the appropriate condition is

$$v_I \varepsilon_{s,f} C_{si,f} = J_{si,f} + r_{si}, \tag{66}$$

with v_I = interface velocity, $\varepsilon_{s,f}$ = volume fraction of solid = 1-n, $C_{si,f}$ = solids density, $J_{si,f}$ = flux of solids towards the interface, and r_{si} = rate of attachment/detachment of solids from the interface. From the derivation above the solids flux is given by

$$J_{si,f} = (1-n) C_S V_{(L_f)}, \tag{67}$$

so that given some r_{si},the interface velocity can be determined.

NUTRIENT DIFFUSION WITHIN THE BIOFILM

General Diffusion Equation

Referring to figure 7, the mass flux is defined in terms of a Fickian diffusion process, i.e., flux = $j = D_b \frac{\partial(nC_b)}{\partial z}$, and the mass balance on the control volume is

$$\begin{aligned} \frac{\partial(nC_b)}{\partial t} A\Delta z &= j_{in} - j_{out} - \text{reaction} \\ &= AD_b \left.\frac{\partial(nC_b)}{\partial z}\right|_{z+\Delta z} - AD_b \left.\frac{\partial(nC_b)}{\partial z}\right|_{z} - rA\Delta z \end{aligned} \tag{68}$$

Since the void fraction (n) is constant, it can be taken out of the derivatives

$$nA\Delta z \frac{\partial C_b}{\partial t} = nAD_b \left.\frac{\partial C_b}{\partial z}\right|_{z+\Delta z} - nAD_b \left.\frac{\partial C_b}{\partial z}\right|_{z} - rA\Delta z \tag{69}$$

Dividing equation 69 by Δz and taking the limit as $\Delta z \rightarrow 0$ gives the following result for the flux terms:

$$\begin{aligned} \lim_{\Delta z \to 0} \frac{nAD_b \left.\frac{\partial C_b}{\partial z}\right|_{z+\Delta z} - nAD_b \left.\frac{\partial C_b}{\partial z}\right|_{z}}{\Delta z} &= \lim_{\Delta z \to 0} \frac{f(z+\Delta z) - f(z)}{\Delta z} \\ = \frac{\partial f(z)}{\partial z} &= \frac{\partial}{\partial z}\left[nAD_b \frac{\partial C_b}{\partial z} \right] \end{aligned} \tag{70}$$

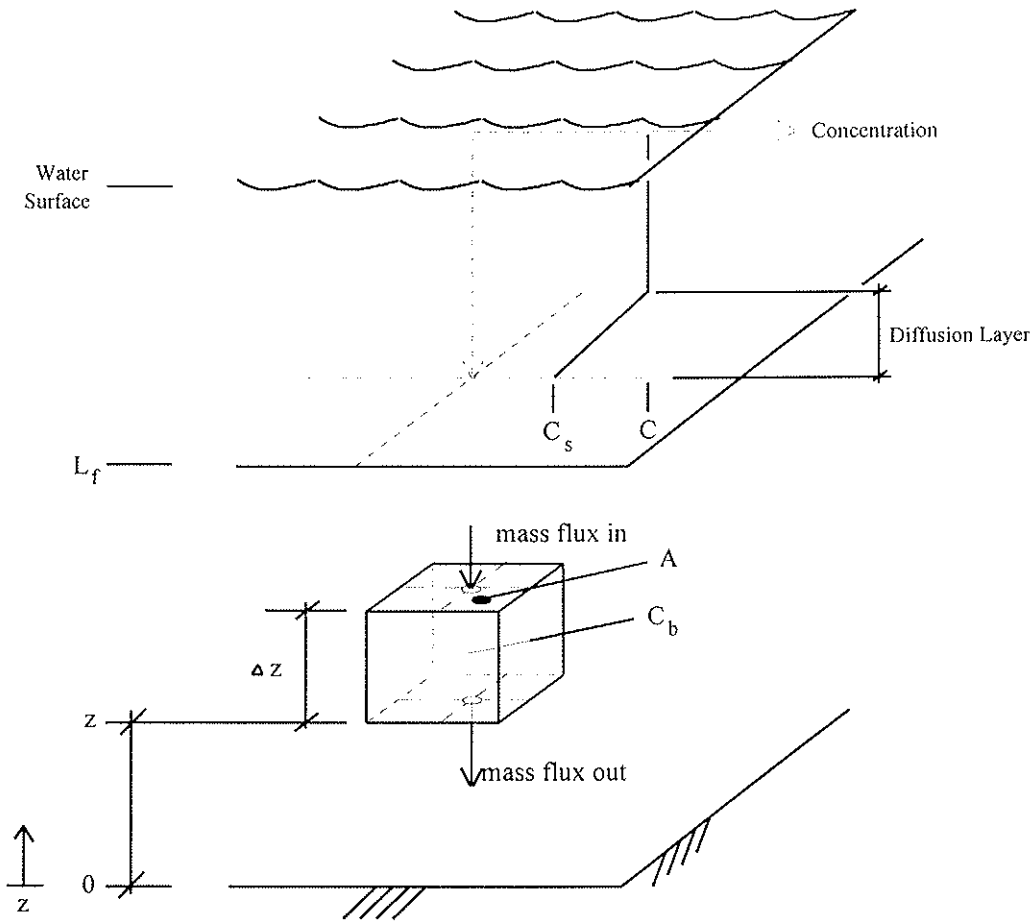

Figure 7: Definition diagram for biofilm diffusion model equations. A control volume located between a solid substrate (z = 0) and the biofilm surface (z = L_f) has a length (Δz) and a surface area (A). A diffusion layer exists in the water column, that can restrict the concentration of substrate (C_s) at the biofilm surface. The plot of concentration vs. depth illustrates this. The rate of diffusion through this layer is influenced by the bulk water concentration (C) and C_s.

Equation 69 then becomes

$$n\frac{\partial C_b}{\partial t}A = \frac{\partial}{\partial z}\left[nAD_b\frac{\partial C_b}{\partial z}\right] - rA\,. \qquad (71)$$

If A, n, and D_b are considered constant throughout the biofilm and dividing by A gives the final result

$$n\frac{\partial C_b}{\partial t} = nD_b\frac{\partial^2 C_b}{\partial z^2} - r \qquad (72)$$

with the following boundary conditions:

$$D_b n \frac{\partial C_b}{\partial z} = 0 \quad \text{for} \quad z = 0$$
$$C_b = C_{surf} \quad \text{for} \quad z = L_f \tag{73}$$

The boundary condition at z=0 is for an impervious boundary (Neuman boundary condition), and that at $z=L_f$ is for a prescribed concentration (Dirichlet boundary condition). Note, the volumetric portion of fluid (n) is not needed for the boundary condition at $z = L_f$, since C_b is the concentration in the fluid fraction.

Rate Equations for Nutrients

Note, in the following rate equations, losses are expressed as positive terms and sources as negative terms. This is a result of the definition of the local source-sink rate, where the value of r is subtracted from the net accumulation rate.

Dissolved Phosphorus

For dissolved phosphorus, the local reaction rate is governed by uptake due to algae growth and production due to organic matter decay.

$$r = \mu_1 (1-n) C_S f_1 \alpha_{1,P} - k_{org} n C_{org} \alpha_{org,P} \tag{74}$$

Organic Phosphorus

Organic phosphorus is handled through organic matter, such that

$$C_{orgP} = k_{org} \alpha_{org,P} n C_{org} \tag{75}$$

This is used to convert organic matter concentrations at the biofilm surface that exchange with the water column. Typically, organic phosphorus is used in water column transport models.

Soluble Organic Matter

The local rate is a function of the intrinsic organic matter decay rate and the rate of organic production from algae. Note the latter actually originates from algal respiration.

$$r = k_{org} n C_{org} - \rho_1 (1-n) C_S f_1 \tag{76}$$

Ammonia

The local ammonia conversion rate is function of algal uptake, decay of organic matter, and oxidation to nitrite.

$$r = \mu_1 (1-n) C_S f_1 \alpha_{1,N} N_{pref} - k_{org} n C_{org} \alpha_{org,N} + k_{NH3} n C_{NH3} \tag{77}$$

where

$$N_{pref} = \frac{P_f nC_{NH3}}{P_f nC_{NH3} + (1 - P_f) nC_{NO3}} \quad (78)$$

Nitrite

The local nitrite conversion rate depends on oxidation of ammonia and nitrite, itself, as well as denitrification which can occur in regions of anoxia.

$$r = -k_{NH3} nC_{NH3} + k_{NO2} nC_{NO2} + k_{deNO2} nC_{NO2} \quad (79)$$

Nitrate

The local nitrate conversion rate is a function of oxidation from nitrite, algal uptake, and denitrification.

$$r = \mu_1 (1 - n) C_S f_1 \alpha_{1,N} \{1 - N_{pref}\} - k_{NO2} nC_{NO2} + k_{deNO3} nC_{NO3} \quad (80)$$

Oxygen

The local oxygen utilization and production rate is a result of organic decay, algal growth, respiration and mortality, oxidation of NO_2-N and NO_3-N.

$$\begin{aligned} r = {} & k_{org} nC_{org} \beta_{org,O2} - \beta_{\mu,O2} \mu_1 (1 - n) C_S f_1 + \beta_{\rho,O2} \rho_1 (1 - n) C_S f_1 \\ & + \beta_{m,O2} m_1 f_d (1 - n) C_S f_1 + k_{NH3} nC_{NH3} \beta_{NH3,O2} + k_{NO2} nC_{NO2} \beta_{NO2,O2} \end{aligned} \quad (81)$$

SPATIAL TRANSFORMATIONS OF GROWTH AND DIFFUSION EQUATIONS

Spatial transformation of the growth and diffusion equations allows simplified handling of the numerical method when the location of a boundary is varying with time. This is the case for a biofilm, where as growth occurs, the biofilm-water interface moves away from the substrate at a velocity governed by the growth rate within the biofilm. The spatial transformation is essentially a non-dimensionalization of the spatial variable (z).

Defining a new spatial variable (z′) as

$$z' = \frac{z}{L_f(t)} \text{ and} \quad (82)$$

the time variable as

$$t' = t \quad (83)$$

provides the basis for the transformation. Derivatives of equations 82 and 83 are then taken with respect to z and t and give the following results:

$$\frac{\partial z'}{\partial z} = \frac{\partial}{\partial z}\left[\frac{z}{L_f(t)}\right] = \frac{1}{L_f(t)} \tag{84}$$

$$\frac{\partial z'}{\partial t} = \frac{\partial}{\partial t}\left[zL_f^{-1}(t)\right] = -\frac{z}{L_f^2(t)}\frac{dL_f(t)}{dt}$$

$$= -\frac{z'L_f(t)}{L_f^2(t)}\frac{dL_f(t)}{dt} = -\frac{z'}{L_f(t)}\frac{dL_f(t)}{dt} \tag{85}$$

$$\frac{\partial t'}{\partial z} = \frac{\partial t}{\partial z} = 0 \tag{86}$$

$$\frac{\partial t'}{\partial t} = \frac{\partial t}{\partial t} = 1 \tag{87}$$

A chain rule is applied to some property ( ) = f(z′,t′) where z′ = g(z,t) and t′ = h(z,t), with the object of finding $\partial(\,)/\partial z$ and $\partial(\,)/\partial t$. These operations are shown in equations 88 and 89 below.

$$\frac{\partial()}{\partial z} = \frac{\partial()}{\partial z'}\frac{\partial z'}{\partial z} + \frac{\partial()}{\partial t'}\frac{\partial t'}{\partial z} = \frac{\partial()}{\partial z'}\frac{1}{L_f(t)} + \frac{\partial()}{\partial t'}\cdot 0$$

$$= \frac{1}{L_f(t)}\frac{\partial()}{\partial z'} \tag{88}$$

$$\frac{\partial()}{\partial t} = \frac{\partial()}{\partial t'}\frac{\partial t'}{\partial t} + \frac{\partial()}{\partial z'}\frac{\partial z'}{\partial t} = \frac{\partial()}{\partial t'} - \frac{\partial()}{\partial z'}\left[\frac{z'}{L_f(t)}\frac{dL_f(t)}{dt}\right] \tag{89}$$

Finally, these are applied to the growth equations and the general diffusion equation developed above, i.e., equations 64, 65, and 72, respectively.

Growth Equations

First the velocity equation 52 must be transformed. Substitute the spatial transform equation 82 into the integration limits.

$$V_{(z')} = \int_0^{z'L_f}\left\{\mu_1(\zeta') - \rho_1 - m_1 f_d\right\}f_1(\zeta')d(\zeta'L_f)$$

$$= L_f\int_0^{z'L_f}\left\{\mu_1(\zeta') - \rho_1 - m_1 f_d\right\}f_1(\zeta')d\zeta' \tag{90}$$

Since L_f is not a variable and is not a function of space, it can be taken out of the integral. For algal growth (equation 64), substituting the spatial transformations gives the following for algae (subscript = 1):

$$\frac{\partial(f_{1(z')})}{\partial t'} - \left\{\frac{z'}{L_f(t)}\frac{dL_f(t)}{dt}\right\}\frac{\partial(f_{1(z')})}{\partial z'} = (\mu_{1(z')} - \rho_1 - m_1)f_{1(z')}$$
$$- \left\{\frac{1}{L_f(t)}\frac{\partial(f_{1(z')})}{\partial z'}\right\}V_{(z')} \qquad (91)$$
$$- f_1^2{}_{(z')}(\mu_{1(z')} - \rho_1 - m_1 f_d)$$

Rearranging and combining terms gives the final transformed equation for algae:

$$\frac{\partial(f_{1(z')})}{\partial t'} = (\mu_{1(z')} - \rho_1 - m_1)f_{1(z')}$$
$$- \frac{1}{L_f(t)}\left\{V_{(z')} - z'\frac{dL_f(t)}{dt}\right\}\frac{\partial(f_{1(z')})}{\partial z'} \qquad (92)$$
$$- f_1^2{}_{(z')}(\mu_{1(z')} - \rho_1 - m_1 f_d)$$

Using the same steps for inert material (equation 65), its final transformed equation results:

$$\frac{\partial(f_{3(z')})}{\partial t'} = m_1(1 - f_d)f_{1(z')}$$
$$- \frac{1}{L_f(t)}\left\{V_{(z')} - z'\frac{dL_f(t)}{dt}\right\}\frac{\partial(f_{3(z')})}{\partial z'} \qquad (93)$$
$$- f_{3(z')}f_{1(z')}(\mu_{1(z')} - \rho_1 - m_1 f_d)$$

Diffusion Equation

To better illustrate the transformation steps, equation 71 is used after dividing through by A.

$$n\frac{\partial C_b}{\partial t} - n\frac{\partial C_b}{\partial z'}\left\{\frac{z'}{L_f(t)}\frac{dL_f(t)}{dt}\right\}$$
$$= \frac{1}{L_f(t)}\frac{\partial}{\partial z'}\left\{nD_b\frac{1}{L_f(t)}\frac{\partial C_b}{\partial z'}\right\} - r \qquad (94)$$

Expanding the derivatives on the right-hand-side

$$n\frac{\partial C_b}{\partial t} - n\frac{\partial C_b}{\partial z'}\left\{\frac{z'}{L_f(t)}\frac{dL_f(t)}{dt}\right\}$$
$$= \frac{n}{L^2{}_f(t)}\frac{\partial(D_b)}{\partial z'}\frac{\partial C_b}{\partial z'} + \frac{nD_b}{L^2{}_f(t)}\frac{\partial^2 C_b}{\partial z'^2} - r \qquad (95)$$

Since it is assumed that D_b is constant, the first term of the right-hand-side goes to zero, and the final transformed equation is obtained:

$$n\frac{\partial C_b}{\partial t'} - n\frac{\partial C_b}{\partial z'}\left\{\frac{z'}{L_f(t)}\frac{dL_f(t)}{dt}\right\} = \frac{nD_b}{L^2{}_f(t)}\frac{\partial^2 C_b}{\partial z'^2} - r \qquad (96)$$

It is interesting to note that the transformed diffusion equation 96 is an advection-diffusion equation with a negative velocity. The boundary conditions must also be transformed, which results in the following equations:

$$\begin{aligned} \frac{D_b n}{L_f(t)}\frac{\partial C_b}{\partial z'} &= 0 \qquad \text{for} \quad z'L_f(t) = 0 \\ C_b &= C_{surf} \qquad \text{for} \quad z'L_f(t) = L_f(t) \end{aligned}, \qquad (97)$$

which can be reduced to the following form:

$$\begin{aligned} \frac{D_b n}{L_f(t)}\frac{\partial C_b}{\partial z'} &= 0 \qquad \text{for} \quad z' = 0 \\ C_b &= C_{surf} \qquad \text{for} \quad z' = 1 \end{aligned} \qquad (98)$$

NUMERICAL SOLUTION OF BIOFILM EQUATIONS

A finite element scheme is used to solve the growth equations for live biomass, inert material, and nutrient and product diffusion. Only the final numerical equations will be presented, since the development is rather extended. More detail can be found in Breithaupt (1995). The diffusion equation expressed in terms of finite elements is given by the following with j = 1,P and P = number of nodes.

$$\sum_{k=1}^{P} M_{j,k}\frac{\partial C_b{}^k}{\partial t} + \sum_{k=1}^{P} K_{j,k}C_b^k = F_j$$

where

$$\begin{aligned} M_{j,k} &= \int_0^1 N_j n N_k\, dz \\ K_{j,k} &= \int_0^1 \left\{ -\left\{\frac{z}{L_{f(t)}}\frac{dL_{f(t)}}{dt}\right\} n N_j \frac{\partial N_k}{\partial z} + \frac{nD_b}{L^2{}_{f(t)}}\frac{\partial N_j}{\partial z}\frac{\partial N_k}{\partial z} + N_j r N_k \right\} dz \\ F_j &= -\int_0^1 N_j S\, dz + N_1 Q_{(z_1)} + N_p Q_{(z_p)} \\ C_b^k &= \begin{bmatrix} C_b^1 \\ C_b^2 \\ \vdots \\ C_b^P \end{bmatrix} \end{aligned} \qquad (99)$$

Note that $z = z'$ for equation 99 - 102. N_n is a basis or weighting function essential to the finite element method, with n being a dummy variable for j or k. For the growth equations, the following finite element representations apply.

$$\sum_{k=1}^{P} M_{i,j,k} \frac{\partial f_{i,k}}{\partial t} + \sum_{k=1}^{P} K_{i,j,k} f_{i,k} = F_{i,j} \text{ , with } i = 1,3 \tag{100}$$

For the algal component (i = 1), the terms of (8) are expressed as follows

$$\begin{aligned}
M_{1,j,k} &= \int_0^1 N_j N_k dz \\
K_{1,j,k} &= -\int_0^1 N_j(\mu_1(z) - \rho_1 - m_1) N_k dz + \int_0^1 N_j \frac{1}{L_f(t)} \left\{ V(z) - z \frac{dL_f(t)}{dt} \right\} \frac{\partial N_k}{\partial z} dz \\
&\quad + \int_0^1 N_j(\mu_1(z) - \rho_1 - m_1 f_d)\left(N_k f_{1,k}\right)^* N_k dz \\
F_{1,j} &= 0 \\
f_{1,k} &= \begin{bmatrix} f_{1,1} \\ f_{1,2} \\ \vdots \\ f_{1,P} \end{bmatrix}
\end{aligned} \tag{101}$$

while for the inert component (j = 3) the terms are

$$\begin{aligned}
M_{3,j,k} &= \int_0^1 N_j N_k dz \\
K_{3,j,k} &= \int_0^1 N_j \frac{1}{L_f(t)} \left\{ V(z) - z \frac{dL_f(t)}{dt} \right\} \frac{\partial N_k}{\partial z} dz \\
&\quad + \int_0^1 N_j f_1(z)(\mu_1(z) - \rho_1 - m_1 f_d) N_k dz \\
F_{3,j} &= \int_0^1 N_j m_1 (1 - f_d) f_{1,k} dz \\
f_{3,k} &= \begin{bmatrix} f_{3,1} \\ f_{3,2} \\ \vdots \\ f_{3,P} \end{bmatrix}
\end{aligned} \tag{102}$$

The time derivative terms are solved using a Crank-Nicholson solution method. Since the equations are non-linear, a Newton-Raphson technique is used to iterative to a solution. In general if a system of equations is being solved involving multiple variables, $\bar{x}_1 \quad \bar{x}_2 \quad \cdots \quad \bar{x}_k$, the Newton-Raphson method is described by the following

$$\frac{\partial q_i^{(n-1)}}{\partial x_j} \Delta x_j \quad = \quad - q_j^{(n-1)}, \quad i, j = 1, 2, \ldots, k \tag{103}$$

with Δx_j being the change from iteration to the next, $\frac{\partial q_i^{(n-1)}}{\partial x_j}$ is the Jacobian matrix of the function r evaluated at the n-1 iterate, and $q_j^{(n-1)}$ is the vector valued function evaluated at the n-1 iterate. After each iteration, the variables are updated by

$$x_j^{(n)} \quad = \quad x_j^{(n-1)} + \Delta x_j \, , \; j = 1, 2, \ldots, k \, . \tag{104}$$

For the problem at hand, there are three sets of equations (k = 3): algae growth, inert material growth, and diffusion transport of nutrients. These are represented as follows

$$\begin{aligned} q_{alg} &= g(f_1, f_3, C_i) \\ q_{int} &= g(f_1, f_3, C_i) \\ q_{nut,i} &= g(f_1, f_3, C_i) \end{aligned} \tag{105}$$

where alg, int, and nut represent the three types of equations, i = the index for a nutrient constituent.

RUSSIAN RIVER MODELING

The Russian River is located approximately 50 miles north of the city of San Francisco (figure 3). The watershed it drains is located in the Coast Range near the northwest coast of California. It is nearly 160 kilometers in length from its mouth at the Pacific Ocean to the source of summer flow at Coyote Dam and Lake Mendocino. Within its basin are located the cities of Santa Rosa and Ukiah and several small towns, including Cloverdale, Healdsburg, Sebastapol, and Guerneville. Wastewater emissions from these communities can begin only after the fall or winter flows first exceed 1000 cfs and must terminate by mid-May of each year. Summer wastewater flows are stored and/or used for irrigation.

The greatest concern is over Santa Rosa's emission. The wastewater is treated to a high degree for biochemical oxygen demand (BOD) removal and a nitrification process was added to prevent toxicity problems from un-ionized ammonia. However, the nitrate levels (NO_3) have increased from the oxidation of ammonia. The emission is actually to a small stream (Laguna de Santa Rosa) that is tributary to the Russian River. The confluence is approximately 38 kilometers above the Russian River's mouth. One important issue is the effect of the emission on the algal growth in the lower river, as well as the Laguna de Santa Rosa. As noted earlier in the report (table 1), *Cladophora* biomass densities up to 40 gm DW m^{-2} were observed at Midway Beach during early May, 1994. By late May the population was in drastic decline, being essentially zero at Odd Fellows. Visual observations (no measurement) were made in August, 1994

To simulate attached filamentous algal growth, the numerical solution methodology discussed above was added to the newly developed model RMA-4q. RMA-4q has been developed in a parallel project as a general purpose 1 and 2D water quality/ecological model with a structure designed to permit easy addition of new constituent relationships. It solve the transport equations using the finite element method. The benthic algae equations solve for growth and interactions at fixed points, since there is no transport involved. These points are taken as the finite element nodes. Values at points between the nodes can be interpolated using the interpolation functions inherent in the finite element method. Model parameters for benthic algal growth are specified nodal, with global values specified and differences from these defined by different node types.

An initial examination of the model was done using a preliminary geometry developed for the Russian River. This results are not for a calibrated model but are solely to indicate attached filamentous algae response and effects under varying but typical hydraulic and water quality conditions. Work continues on improving the system's geometry, and more tests and a calibrated model for the Russian River will be forthcoming.

METHODOLOGY

A test of the filamentous algae model was performed using the Russian River's geometry. The geometry was developed from cross-sections measured by the Sonoma Country Water Agency. The upper boundary for the model was taken at approximately river kilometer (rk) 47.8. This corresponds approximately to the location of the Healdsburg

recreation dam. The measured cross-sections were fitted to trapezoidal sections, then a cubic spline interpolation was done between adjacent cross-sections at half-kilometer intervals. These then described the cross-sections at corner nodes. Note that within the RMA models a linear interpolation is used for the mid-side node cross-sections.

The test was designed to demonstrate the growth of filamentous attached algae (BA) with a constant mass flux (mass/time) of nutrient (nitrate) to the river. Temperature and dissolved oxygen (DO) were also simulated. Besides computing the daily variation of temperature, the temperature routine computes solar radiation needed for benthic algal growth. Nitrate was selected as the primary nutrient, since observed nitrogen:phosphorus ratios for the Russian River indicate nitrogen is limiting.

The flow at the upstream river boundary was varied to simulate recession between storms, followed by storm flow with subsequent recession. The total length of the simulation is 720 hours (30 days). Flow began at 6.0 $m^3 s^{-1}$ (210 cfs) and decreased at a constant rate to 3.0 $m^3 s^{-1}$(105 cfs) at hour 504. At hour 576 flow reached a peak of 28.0 $m^3 s^{-1}$(980 cfs) after increasing at a constant rate. Storm flow ended at hour 696 with a flow of 6.0 $m^3 s^{-1}$ (210 cfs) and receded at the same rate as at the beginning of the simulation until hour 720 when the simulation was terminated. Nitrate concentration varied with flow, since the mass loading was a constant 0.6 gm NO3-N s^{-1}, which gives a concentration of 0.1 mg NO3-N L-1 at 6 $m^3 s^{-1}$. Temperature boundary conditions were varied over a daily cycle. An initial run was made at low flow with a constant temperature boundary condition. Cooling or heating took place so that at some distance away from the boundary an "equilibrium" condition was reached. These temperatures were then used to reflect the daily variation expected at the system boundary. The rates and parameters used for benthic algae in the simulation are listed in table 4. For the purposes of this application the following detachment relation was used

$$r_d = 2x10^{-11} u^{5.4547}$$

with r_d = detachment rate (day^{-1}) and u = velocity above the bed (cm s^{-1}).

Results are reported at twelve hour intervals and correspond to midnight and noon. Each of the time history plots reflect this, since solar radiation varies from zero to near maximum, respectively.

Table 4: Rate coefficient and parameter values used in filamentous algae simulation. System geometry is that for the Russian River, CA.

Fraction of benthic algal biomass that is nitrogen	0.085
Fraction of benthic algal biomass that is phosphorus	0.0135
Oxygen production per unit of benthic algae growth (mg mg-1)	1.6
Oxygen uptake per unit of benthic algae respiration (mg mg-1)	2.0
Temperature correction factor for benthic algal growth rate	1.047
Temperature correction factor for benthic algal respiration rate	1.047
Preference for ammonia-N over nitrate-N by benthic algae (range 0.0-1.0)	0.50
Maximum specific growth rate for benthic algae (1/day)	1.0
Respiration rate for benthic algae (1/day)	0.05
Light half-saturation constant for benthic algae	0.004
Nitrogen half-saturation constant for benthic algae	0.03
Phosphorus half-saturation constant for benthic algae	0.02
Maximum density of benthic algae allowed by the habitat (mg m-2)	100

TEMPERATURE

In figure 8, a temperature time history is plotted for river kilometer 26.6. The location corresponds to one of the two regions of the river where attached biomass have been observed to grow. The maximum and minimum temperatures can be seen to gradually increase up to hour 504, when flow started to increase. At this time the flow is near 3 m^3 s^{-1}. A curious feature of the temperature is the longitudinal phasing of temperature variations; the minimum temperature occurs near noon and maximum temperature occurs near midnight. A deep pool upstream of the site reduces heat exchange of the whole water column implying that the temperature variation at rk 26.6 is largely a result of advective transport (figure 9). Warm water added to the pool during the daylight period from heating that occurred in the shallow upstream reaches was transported out of the pool during the dark period. Longitudinal plots of temperature (figure 10) show this phasing occurring along the length of the river. With the river temperature at some locations out of phase with air temperature and solar heating, the oscillations are eventually damped, so that in the river's lower reaches, little diurnal temperature variation occurs. Using a constant temperature boundary condition of 14°C also resulted in temperature being out of phase near rk 26.6 (figure 11). For this the flow was near 6 m^3 s^{-1}. This higher flow causes the phasing to be shifted somewhat downstream. It is not known if this phenomena is real or an artifact of the system's geometry. Cross-section data used to construct the geometry were somewhat sparse, and the influence of one cross-section on adjacent interpolated cross-sections may exaggerate its influence. This needs to be examined further.

BENTHIC ALGAE

Longitudinal plots of benthic algae at selected times are shown in figure 12. Most growth occurs only in certain regions, i.e., rk 32 - 22 and rk 16 - 0. Little growth occurred above rk 32 even though there was adequate nutrient (NO3) available. The figure shows benthic algae densities at hour 492, 12 hours prior to increased flows. At hour 588, near the time of peak flow, biomass densities had declined from detachment above rk 14. Downstream of rk 14 increase in biomass density was still evident in spite of the velocities being near the magnitudes seen near rk 25 (see figure 13). Detachment loss was computed using the following relation derived from the current laboratory experiments

$$d_{afa} = (A_b B_{afa}) 2x10^{-11} v^{5.4547} \qquad (102)$$

where v = velocity in cm s-1 and other terms are as defined earlier. (A power curve relation was found most appropriate, since even at low velocity some detachment was evident in the laboratory experiment.)

Figure 8: Time history plot of temperature at river kilometer 26.6.

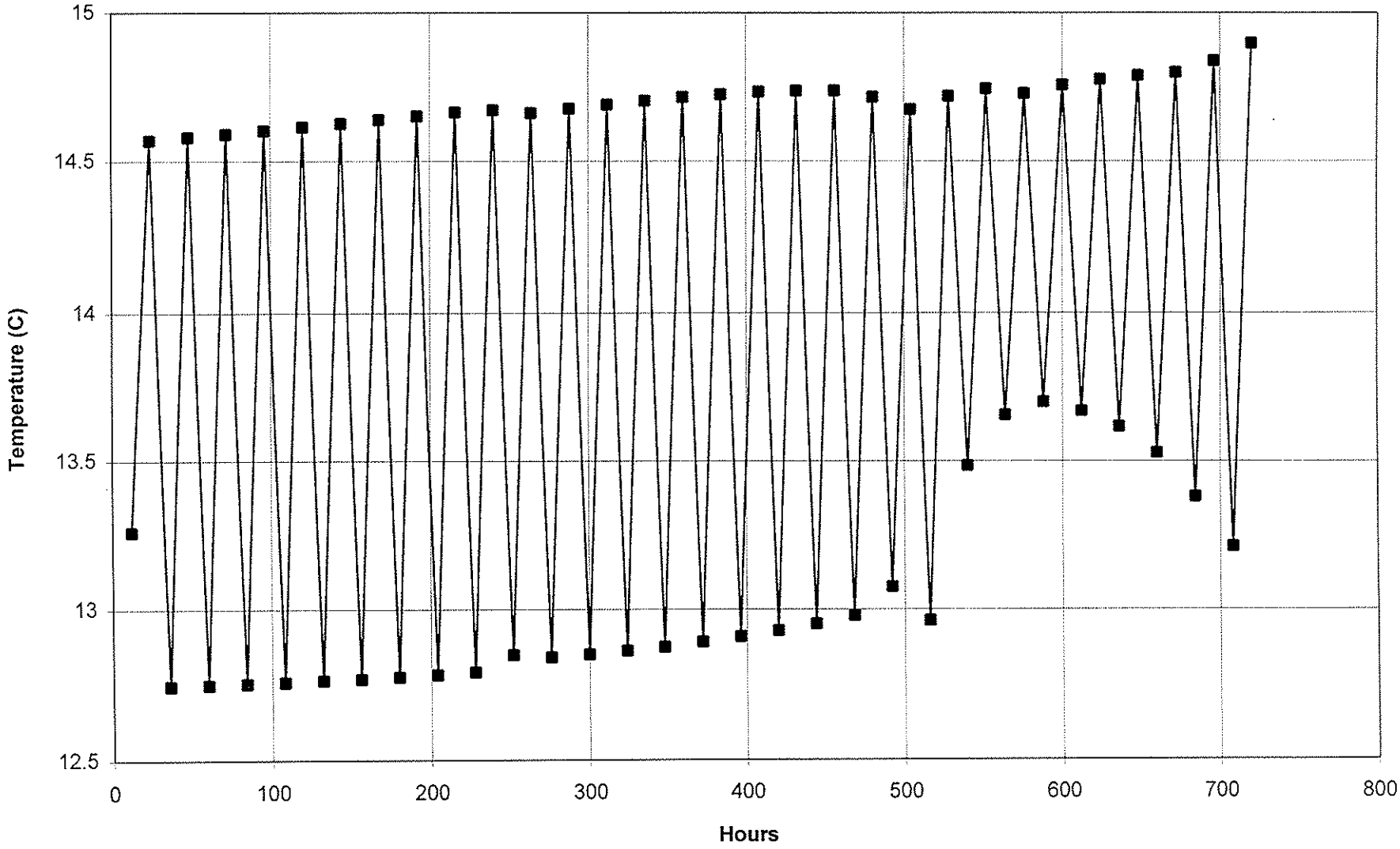

Figure 9: Longitudinal plot of depth at hour 504 immediately prior to the onset of the flood wave.

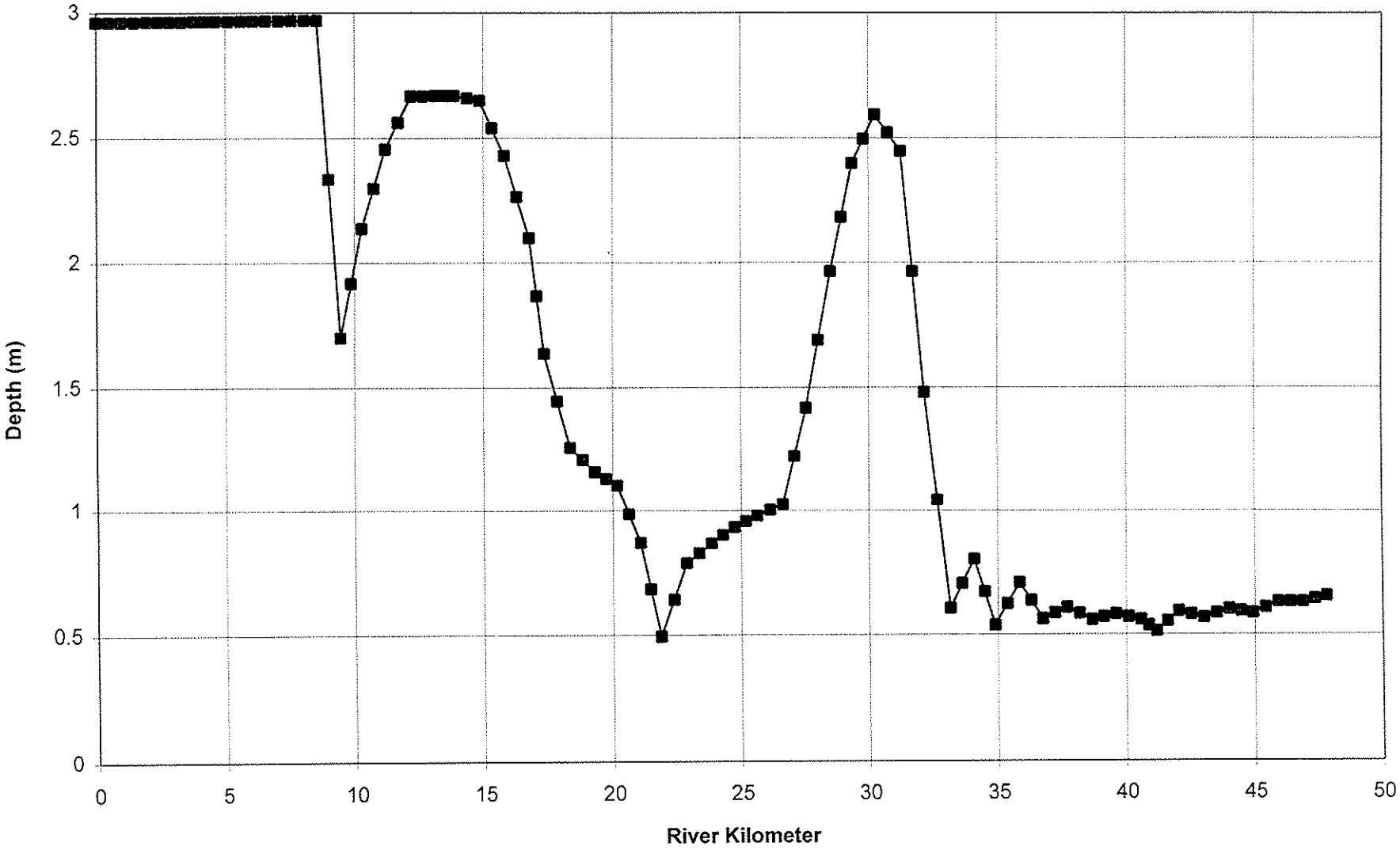

Figure 10: Longitudinal plot of temperature for a Russian River geometry. The times plotted are prior to the onset of the flood wave and after the influence of initial conditions is done.

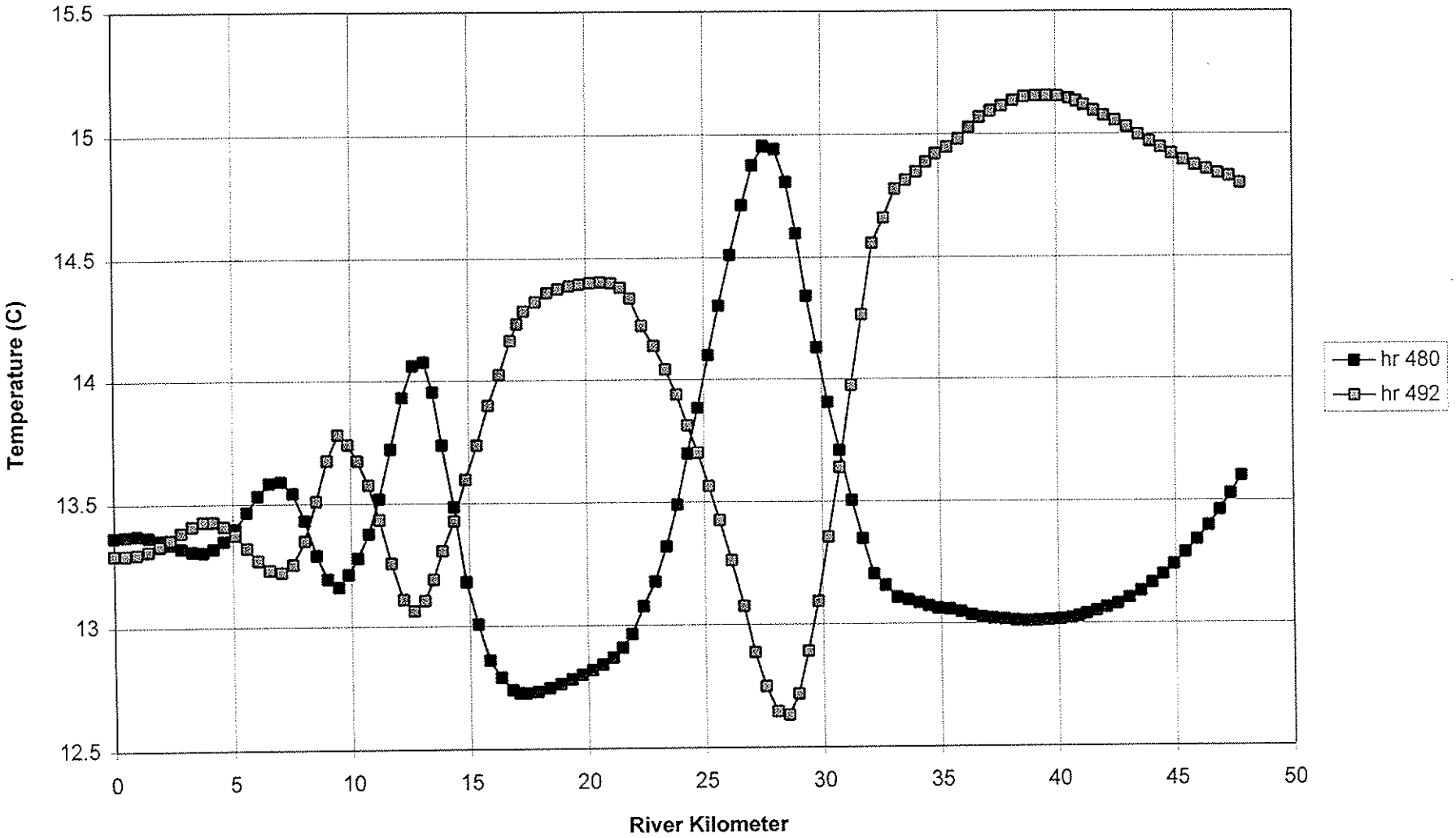

Figure 11: Longitudinal plot for temperature with a constant boundary condition. The geometry is for the Russian River.

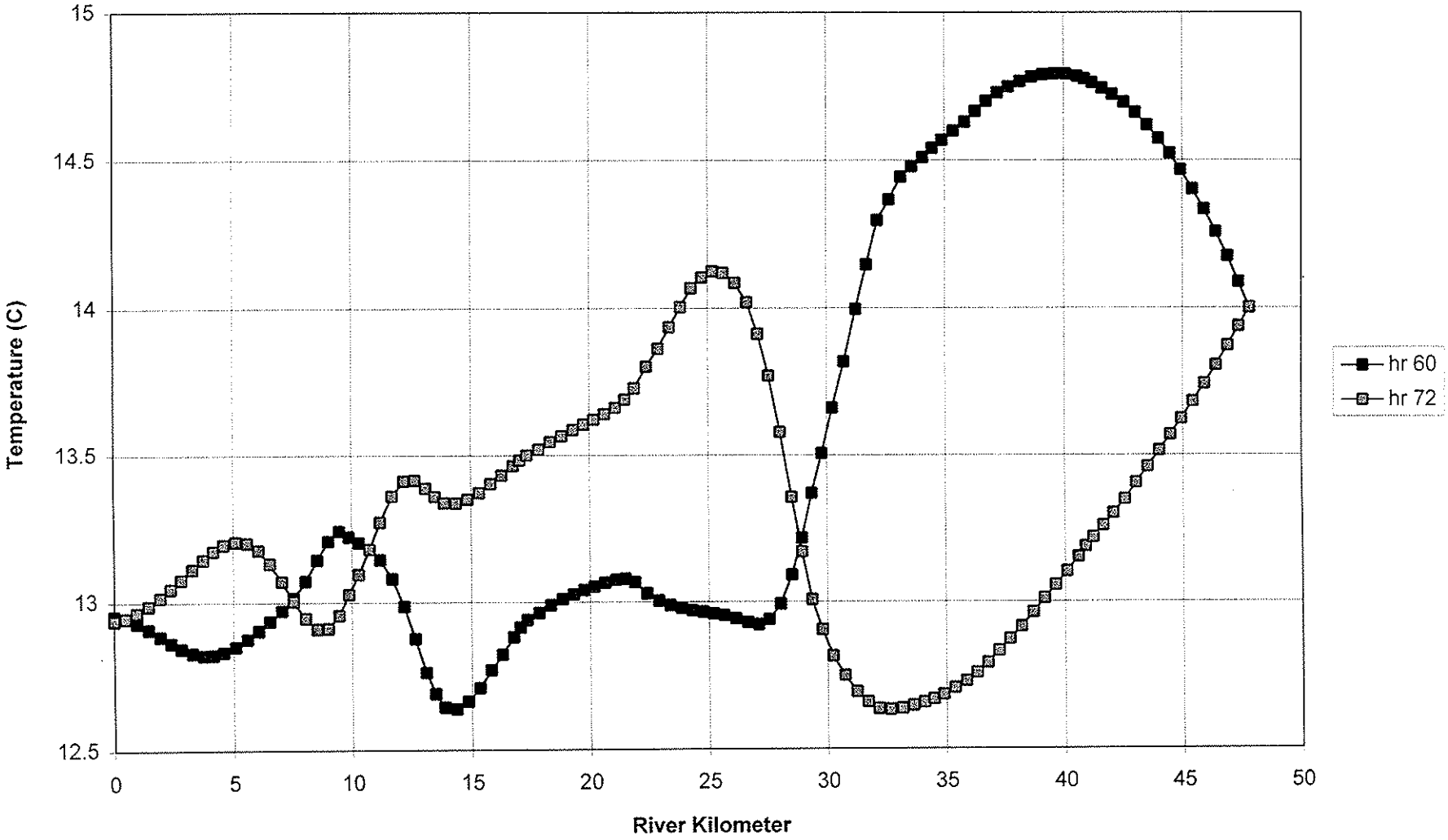

Figure 12: Longitudinal plot of benthic algae shortly before and during the flood wave (hours 492 and 588 respectively) and at the end of the simulation (hour 720).

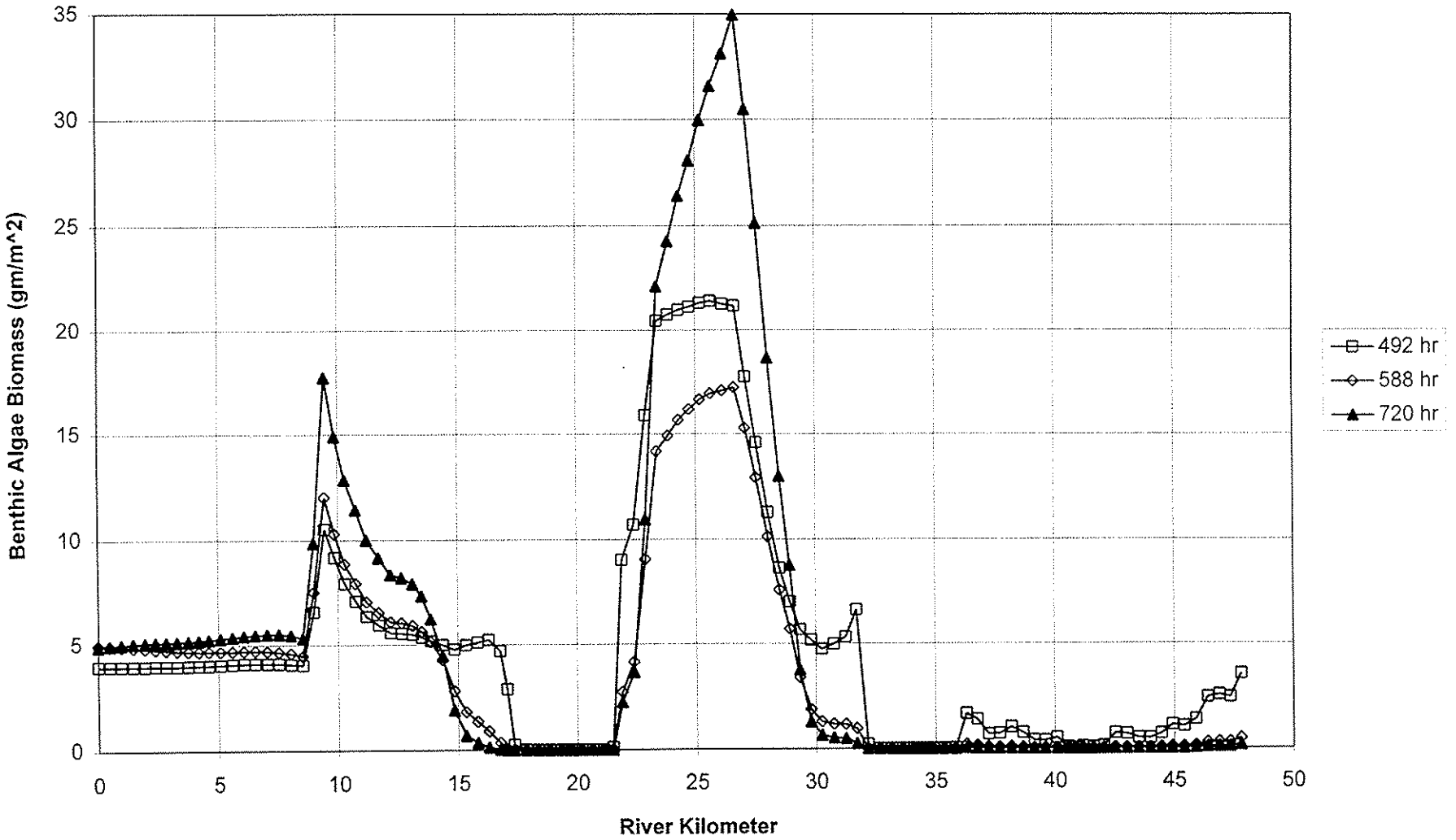

Figure13: Longitudinal plot of velocity for a Russian River geometry. Times plotted are for the near the beginning of the simulation (hour 12), shortly before and after onset of the flood wave (hours 492 and 588), and at the end (hour 720).

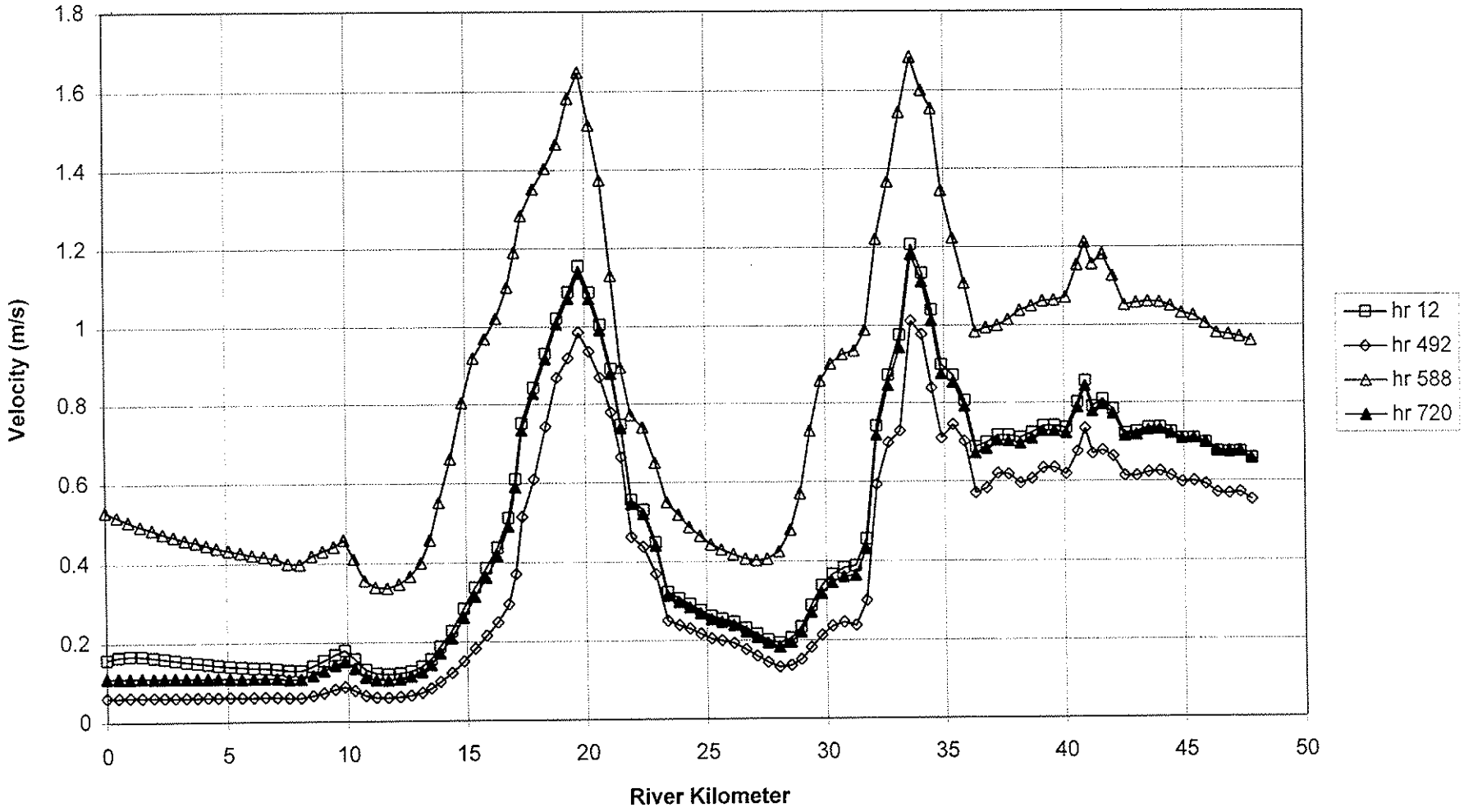

Time history plots at rk 9.4 and 26.6 better illustrate the effects of hydrodynamic detachment and nutrient limitation (figures 14 and 15, respectively). After hour 504 the velocity increases because of the flood wave traveling through the system. At hour 516 the scour rates are 7.8×10-5 and 0.013 gm m-2 day-1 at rk 9.4 and 26.6, respectively. It can be seen in figure 14 that at hour 516 biomass density did not decrease at rk 9.4, while it did at rk 26.6 (figure 15). The difference in detachment rate accounts for this. Later during the period of increasing velocities (hour 564) the detachment rates are 0.126 and 0.172 gm m-2 day-1 for rk 9.4 and 26.6, respectively, giving decreased biomass density at both locations. Note that the appearance of continual growth given by these plots, which are plotted at 12 hour intervals (noon and midnight) is deceptive, since growth occurs only during the daylight period while detachment occurs continuously.

NITRATE

Longitudinal plots of nitrate concentration are plotted in figure 16. The variation in the boundary values is evident by the increasing concentrations at rk 47.8 until hour 504 when concentration decreased, reaching a minimum at hour 576. Since the times plotted are all at the noon hour, the benthic algal uptake of nitrate is seen as troughs in waves traveling through the system. The deep troughs, especially for hour 492, reflect the relatively large biomass densities and long residence times (low velocity), while at hour 588 the higher velocities and short residence times allow less uptake to occur. As velocities decrease further (hour 684) more uptake is evident.

The daily variations in nitrate concentration from benthic algal uptake are readily seen in figure 17 as oscillating concentrations. Uptake is also seen by the decreasing concentrations in downstream locations. Note that rk 47.8 is the upper boundary for this system, and concentrations there are the boundary condition values.

For rk 26.6 variation in nitrate concentration is out of phase with growth from the start of the simulation until near hour 120, when biomass density is relatively small (figure 17). This reflects uptake and travel time upstream. By hour 204 biomass density in the neighborhood of rk 26.6 was significant enough to exert its own influence on nitrate concentration, since the daily variations are in phase with the local growth (solar) cycle.

With increasing velocities and shorter travel times the flood wave causes nitrate concentration to approach that present at the boundary, at least for a short period until the new and decreasing boundary conditions are transported through the system (figure 17). After hour 600 daily variations from nitrate uptake are again evident; however, now rk 9.4 is out of phase with the daily cycle being affected by uptake upstream.

Figure 14: Time history plot of velocity and benthic algae density at river kilometer 9.4.

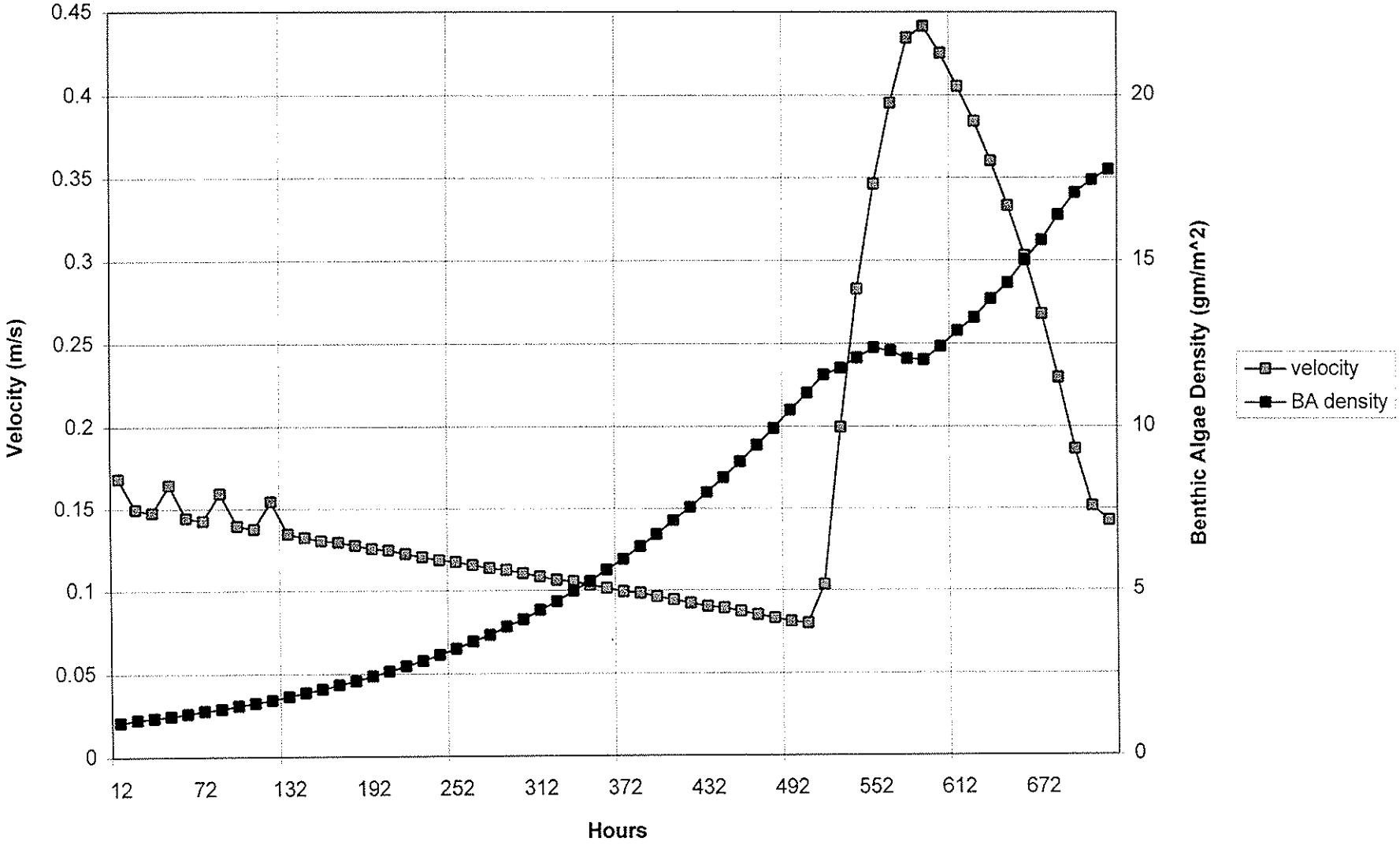

Figure 15: Time history plot of velocity and benthic algae density at river kilometer 26.6.

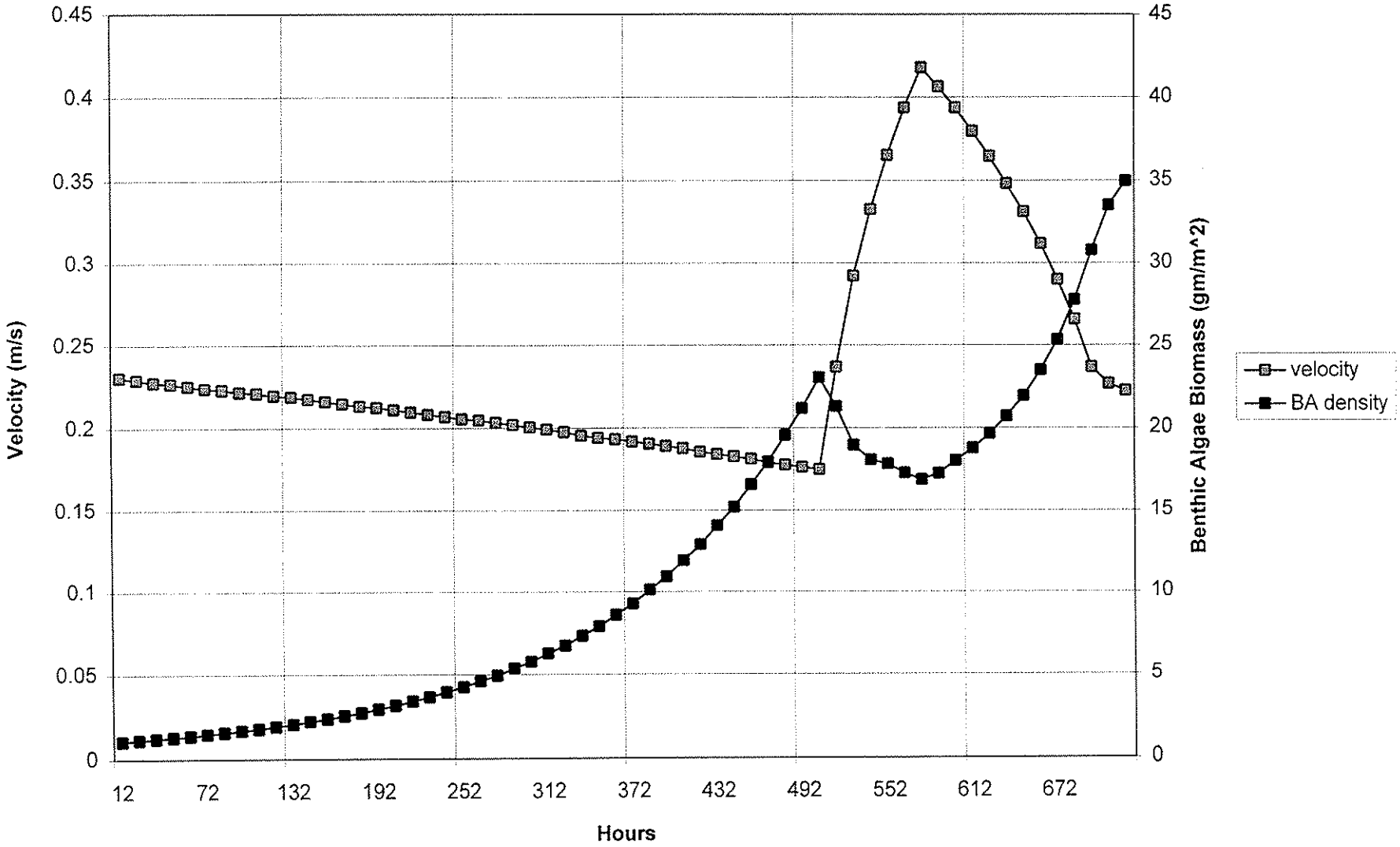

Figure 16: Longitudinal plot of nitrate for a Russian River geometry. Three day intervals are plotted.

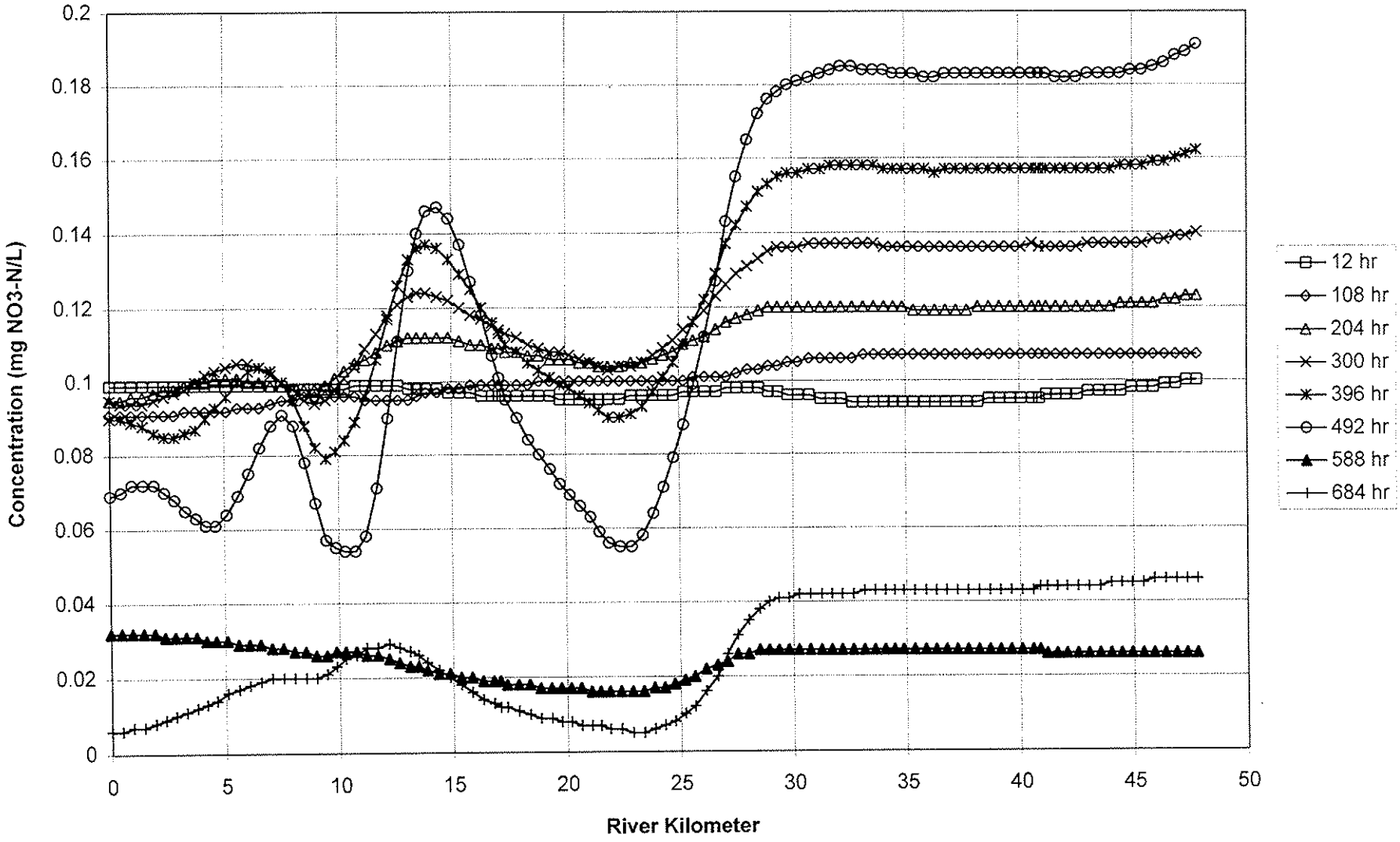

Figure 17: Time history plot of nitrate for a Russian River geometry at river kilometers 47.8, 26.6, and 9.4.

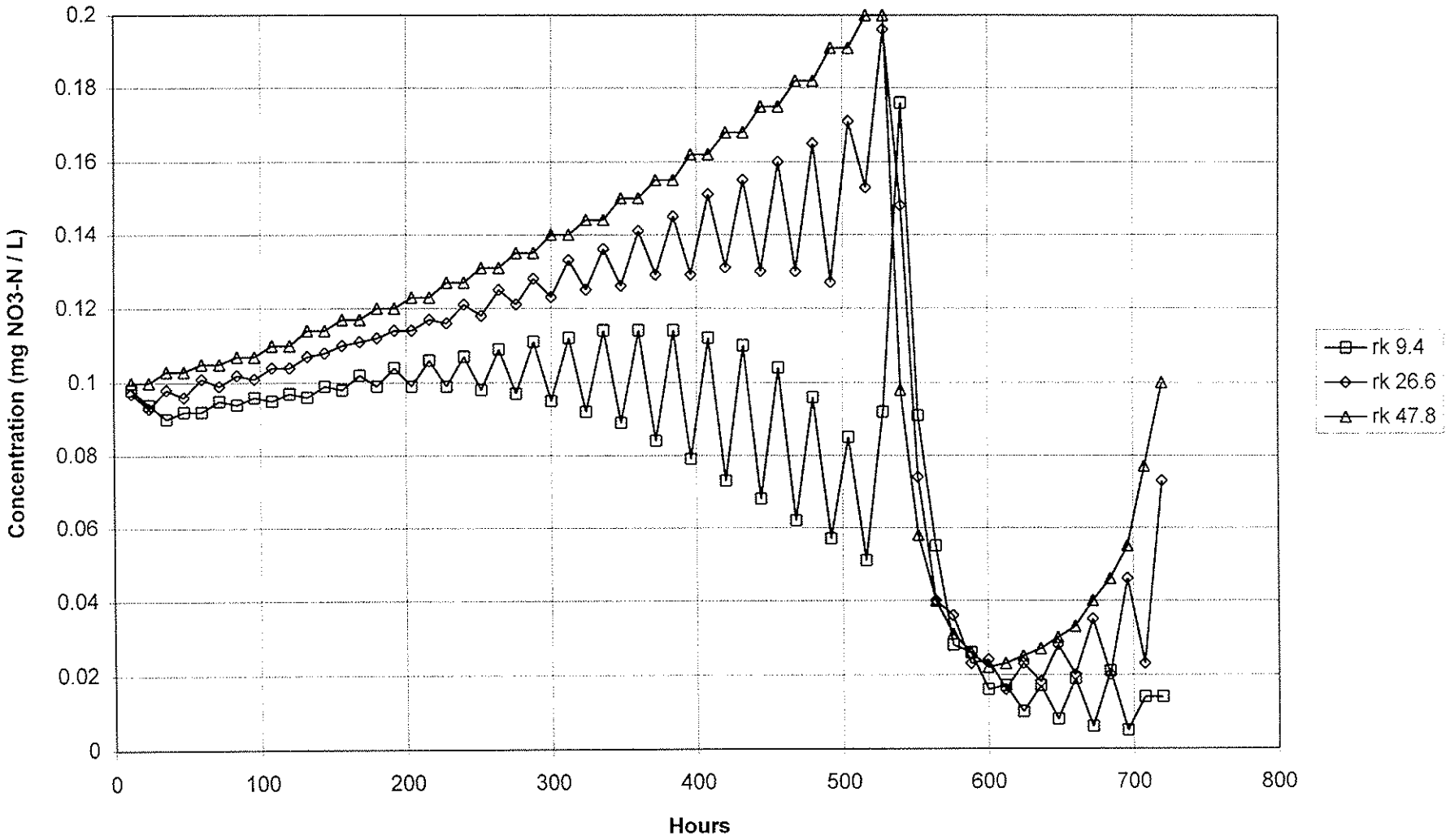

SUMMARY AND CONCLUSIONS

The purpose of this project has been to develop models that simulate benthic algae and their interaction with the water column. The types of benthic algae simulated are classified as attached filamentous algae and perilithic biofilm. These are influenced by different physical processes and require different approaches.

In support of the modeling effort, field and laboratory data were collected on the water quality and benthic algae (*Cladophora*) present in the Russian River, California. Maximum density of *Cladophora* observed in Russian River was 40 gm m^{-2} at Midway Beach (MW). This is less than that seen by Grenney and Kraszewski. (1981), i.e., 100 gm m^{-2}, but MW is located several miles below the Santa Rosa emission point. The laboratory study shows a good relation between velocity and detachment. More data are needed, but length of runs required and obtaining live *Cladophora* are significant impediments. However, this work is an important first step in evaluating hydrodynamic detachment of *Cladophora*.

Model equations for attached filamentous algae are developed as ordinary differential equations. The modified Euler method is used to solve these equations, since interaction data is only known at the beginning and end of a time step. Equations for perilithic biofilm are coupled growth and diffusion equations, and there is a changing matrix thickness (due to algal growth) through which nutrients must be transported before they are used for algal growth. The biofilm equations are solved using the finite element method. The solution of the biofilm equations has significant computational implications, since it must be solved at each gauss point in order to evaluate the exchange with the water column. As a consequence, these equations are more complex than those for attached filamentous algae, since the uptake of nutrient occurs within a matrix of live and inert matter and the nutrients must be transported to the site of uptake by diffusion. In contrast, the filamentous algae (*Cladophora*) remove nutrient within the turbulent zone of the free-flowing fluid; hence no diffusion limitations are assumed to occur. More work is needed to complete the perilithic biofilm model.

Sample application of the equations for attached filamentous algae was presented for the Russian River. Flow and nutrient concentration were varied to simulate a sequence of decreasing base flow, storm flow, and recession. Nutrient concentration at the upstream boundary was varied inversely with the flow, assuming a constant mass loading rate. Attached algal growth occurred in shallow areas with moderate velocity. Where velocity was large, growth did not occur due to hydrodynamic detachment of benthic algae biomass. Where growth occurred during daylight hours, nitrate was removed in proportion to the growth rate. Since growth is a cyclic phenomenon, waves of varying nitrate concentration passed down the system in the direction of flow. A question arose about the correctness of the geometry, which was based on river cross-section data measured by the Sonoma County Water Agency. It is possible that a deep observed cross-section near rk 30 may have biased the interpolation scheme used to estimate cross-sections where data were not available. This bias would extend deep interpolated

cross-sections upstream and downstream farther than actually present. A consequence may be the release of cool water from the deep river reach during the daylight period, which had been added from heat loss in upstream reaches during the previous dark period; storage and release of warm water would also occur during the dark period for the same reasons. This would account for the temperature inversions seen in reaches downstream of rk 30. It is not certain this is correct. Diurnal field data will be examined to evaluate the situation. Also, the geometry will be re-examined and additional cross-section data will be sought to improve the description of the system's geometry.

With this caveat, the attached filamentous algae results are as were intuitively expected. Biomass density increased under favorable growth conditions: low velocity and high nutrient concentrations. When average flow and velocity increased, detachment increased with a concomitant decrease in biomass density. The return of favorable growing conditions again resulted in increasing density.

Nitrate results followed the diurnal variation in attached algal growth: decreasing during the daylight period and increasing during the night. Overall, there is a decrease in concentration as a parcel of water moves downstream. This nitrogen is stored in the attached algae.

RECOMMENDATIONS FOR FUTURE RESEARCH

One purpose of this work has been to extend water quality modeling to include processes which occur on the bed of aquatic systems. By the inclusion of two types of benthic algae (attached filamentous algae and perilithic biofilm), this has been partially accomplished. Aquatic macrophytes are another important component fixed to the bed that interacts with constituents in the water column. A particularly interesting aspect of macrophyte growth may be its effect on system hydraulics. As they grow, fluid friction would increase, reducing velocities in the neighborhood of the macrophyte beds. This process could be important in lake and reservoirs with macrophyte problems and warrants investigation.

The biofilm model developed here focuses on algal growth and conversion to inert material; bacteria and their effects are included implicitly. Future versions of this model should include explicit modeling of bacteria, which can be important in denitrification and conversion of organic matter back to useable nutrients.

Field investigations of both attached filamentous algae and perilithic biofilm are limited by sample collection time and limits the amount of data available for use with the model. The development of methods to rapidly estimate biomass densities for both benthic algae types would be extremely useful. Also, the development of accurate measurement methods of biofilm thickness would improve the applicability of a biofilm such as the one developed in this project.

REFERENCES

American Public Health Agency. 1985. Standard Methods for the Examination of Water and Wastewater.

Atkinson, B. 1974. Biochemical Reactors. Pion Ltd. London.

Auer, M. T. and R. P. Canale. 1982c. Ecological studies and mathematical modeling of *Cladophora* in Lake Huron: 3. The dependence of growth rates on internal phosphorus pool size. J. Great Lakes Res. 8(1):93-99.

Bakke, R., W. G. Characklis, M. H. Turakhia, and A. Yeh. 1990. Modeling a monopopulation biofilm system: *Pseudomonas aeruginosa*. In: Biofilms. Characklis, W. G. and K. C. Marshall (eds.). J. Wiley and Sons. New York.

Bowie, G. L, *et al.* 1985. Rates, Constants, and Kinetic Formulations in Surface Water Quality Modeling, 2nd ed. EPA/600/3-85/040. USEPA Athens, GA.

Breithaupt, S. A. (in draft). An ecological model incorporating benthic algae in an unsteady hydrodynamic and water quality framework. Ph.D. dissertation. Dept. of Civil and Envir. Eng. Univ. of Calif. Davis, Calif.

Canale, R. P. and M. T. Auer. 1982e. Ecological studies and mathematical modeling of *Cladophora* in Lake Huron. 5. Model development and calibration. J. Great Lakes Res. 8(1):112-125.

Corning, K. E., H. C. Duthie, and B. J. Paul. 1989. Phosphorus and glucose uptake by seston and epilithon in boreal forest streams. J. No. Amer. Benthol. Soc. 8(2): 123-133.

Grenney, W. J. and A. K. Kraszewski. 1981. Description and Application of the Stream Simulation and Assessment Model, Version IV (SSAM IV). Cooperative Instream Flow Service Group. Instream Flow Inf. Paper: No. 17. US Fish and Wildlife Service. FWS/0BS-81/46.

Gujer, W. and O. Wanner. 1990. Modeling mixed population biofilms. In: Biofilms, Characklis, W. G. and Marshall, K. C. eds. J. Wiley and Sons. New York.

Haack, T. K and G. A. McFeters, 1982. Nutritional relationships among microorganisms in an epilithic biofilm community. Microbial Ecol. 8:115-126.

King, I. P. and J. F. DeGeorge. 1994. RMA-4q - A Two Dimensional Finite Element Model For Water Quality In Estuaries And Streams - Version 1.0. Dept. Of Civil And Environmental Engineering, University Of California Davis, Ca.

Kissel, J. C., P. L McCarty, and R. L. Street. 1984. Numerical simulation of mixed-culture biofilm. Jour. Env. Eng. ASCE. 110(2): 393-411.

Krenkel P. A. and E. L. Thackston. 1969. Discussion by: Novotny V. 1969. Boundary layer effect on the course of the self-purification of small streams. In: Advances in Water Pollution Research - Proc. 4th Int. Conf. Jenkins, S. H. (ed.) pp.51-53 Pergamnon Press. Oxford.

Novotny V. 1969. Boundary layer effect on the course of the self-purification of small streams. In: Advances in Water Pollution Research - Proc. 4th Int. Conf. Jenkins, S. H. (ed.) pp. 39-50. Pergamnon Press. Oxford.

Rittman, B. E. 1982. The effect of shear stress on biofilm loss rate. Biotech. Bioeng. 24:501-506.

Smith, D. J. 1978. Water Quality for River-Reservoir Systems. Resource Management Associates, Layfayette, CA. Prepared for US Army Corps of Engineers. Hydrologic Engineering Center. Davis, CA.

Stewart, P. S. 1993. A model for biofilm development. Biotech. Bioeng. 41: 111-117.

Trulear, M. G. and W. G. Characklis. 1980. "Dynamics of biofilm processes," Proc. 53rd Ann. Conf. Water Poll. Contr. Fed. Las Vegas, NV. Sept. 1980.

Wetzel, R. G. 1975 Limnology. W. B. Saunders Co. Philadelphia. pp. 393-4.

APPENDIX A

VARIABLE DEFINITIONS USED FOR EQUATION DEVELOPMENT

FILAMENTOUS ALGAE VARIABLE DEFINITIONS

$\mu_{net(t)}$ = net growth from internal processes in response to the nutrient and light regime (day^{-1})
$g_{(t)}$ = grazing losses by aquatic invertebrates and fish (day^{-1})
$d_{(t)}$ = hydrodynamic detachment (gm day^{-1}).
B_{afa} = biomass density of attached filamentous algae (gm m^{-2})
A_b = bed area of the water body (m^2).
d_{afa} = detachment flux caused by drag on the filaments from fluid flow (gm day^{-1})
μ_{max} = maximum specific growth rate for the filamentous algal species (day^{-1})
F_L = Monod light limitation factor (dimensionless)
I = the light intensity at the bed (langleys)
K_L = half-saturation constant for light (langleys)
F_p = Monod phosphorus limitation factor (dimensionless)
P = dissolved orthophosphate concentration near the filamentous algae (mg L^{-1})
K_P = half-saturation coefficient for phosphorus (mg L^{-1})
F_N = Monod nitrogen limitation factor (dimensionless)
N = inorganic nitrogen (nitrate and ammonia) concentration near the filamentous algae (mg L^{-1})
K_N = half-saturation coefficient for nitrogen (mg L^{-1})
ρ = algal respiration rate (day^{-1})
m = algal mortality (day^{-1}).

BIOFILM VARIABLE DEFINITIONS

A = surface area of control volume within the biofilm = CONSTANT (mm^2)
C = bulk fluid nutrient concentration (mg L^{-1})
C_b = nutrient concentration in the fluid volume fraction of the biofilm (mg L^{-1}), so that the concentration over the whole control volume is nC_b.
C_{NH3} = local concentration of ammonia (mg L^{-1})
C_{NO2} = local concentration of nitrite (mg L^{-1})
C_{org} = local concentration of organic matter (mg L^{-1})
C_s = density of the solid fraction (1-n) (mg mm^{-3})
C_{surf} = nutrient concentration at the biofilm-water interface (mg L^{-1})
C_* = light intensity (langleys) or nutrient concentration of P, N, or Si (mg L^{-1}).
D_b = diffusion coefficient within the biofilm (mm^2 day^{-1})
f_d = fraction of organic matter that is readily degradable in the biofilm. For algae these are the respiration and mortality products.
f_k = fraction of kth constituent present in the biofilm
fl(z) = total mass flux at z in the biofilm (mg day^{-1})
F_* = Monod growth factor for light, phosphorus, nitrogen, and silicon, where * = L, P, N, and Si, respectively.
j = mass flux on nutrient due to diffusive transport (mg mm^{-2} day^{-1})

k = 1,2,3 = indices for algae, bacteria, and particulate, inert, organic material, respectively, present in the biofilm

k_{deNO2} = first-order denitrification rate for nitrite (day^{-1})

k_{deNO3} = first-order denitrification rate for nitrate (day^{-1})

k_{NH3} = first-order oxidation rate of ammonia to nitrite (day^{-1})

k_{NO2} = first-order oxidation rate of nitrite to nitrate (day^{-1})

k_{org} = first-order decay rate of organic material (day^{-1})

K_* = half-saturation coefficient for light intensity (langleys) or concentration of P, N, or Si ($mg\ L^{-1}$).

L_f = total depth of the biofilm (mm)

m_1 = mortality rate coefficient for algae resulting in death of cells (day^{-1})

n = volume fraction of voids that is filled with fluid = CONSTANT

N_{pref} = fraction of algal uptake of inorganic nitrogen derived from NH_3-N pool

P_f = preference factor for NH_3-N; ranges from 0.0 to 1.0

r = local rate of change due to biological or chemical processes ($mg\ L^{-1}\ day^{-1}$)

t = time in global coordinate system (day)

t′ = time in transformed coordinate system (day)

V(z) = velocity at distance z in biofilm resulting from growth at locations less than distance z.

X_f = average density of the biofilm = $(1-n)C_s + n\rho_w$ ($mg\ mm^{-3}$)

z = global spatial coordinate normal to the attachment substrate of biofilm (mm)

z′ = transformed spatial coordinate normal to the attachment substrate of biofilm; ranges from 0 to 1.

$\alpha_{1,N}$ = yield coefficient for nitrogen; proportion of algae that is N ($mg\ mg^{-1}$)

$\alpha_{1,P}$ = yield coefficient for dissolved phosphorus; proportion of algae that is P ($mg\ mg^{-1}$)

$\alpha_{org,N}$ = proportion of organic matter that is N ($mg\ mg^{-1}$)

$\alpha_{org,P}$ = proportion of organic matter that is P ($mg\ mg^{-1}$)

$\beta_{org,O2}$ = mass of oxygen consumed per unit of organic matter lost by decay ($mg\ mg^{-1}$)

$\beta_{\mu,O2}$ = mass of oxygen produced per unit mass of algal growth ($mg\ mg^{-1}$)

$\beta_{\rho,O2}$ = mass of oxygen consumed per unit algal mass respired ($mg\ mg^{-1}$)

$\beta_{NH3,O2}$ = mass of oxygen consumed per unit mass of NH_3-N oxidized ($mg\ mg^{-1}$)

$\beta_{NO2,O2}$ = mass of oxygen consumed per unit mass of NO_2-N oxidized ($mg\ mg^{-1}$)

μ_1 = non-linear growth rate for algae after considering nutrient and light limitations (day^{-1})

$\mu_{1,max}$ = maximum non-linear growth rate coefficient for algae (day^{-1})

ρ_1 = respiration rate coefficient for algae resulting in loss of organic material and associated nutrients from cells due to cell maintenance, etc. (day^{-1})

ρ_w = density of water ($mg\ mm^{-3}$)

ζ = dummy variable for biofilm depth (mm)